Article

Current Biology

Resource allocation strategies and mechanical constraints drive the diversification of stick and leaf insect eggs

Graphical abstract

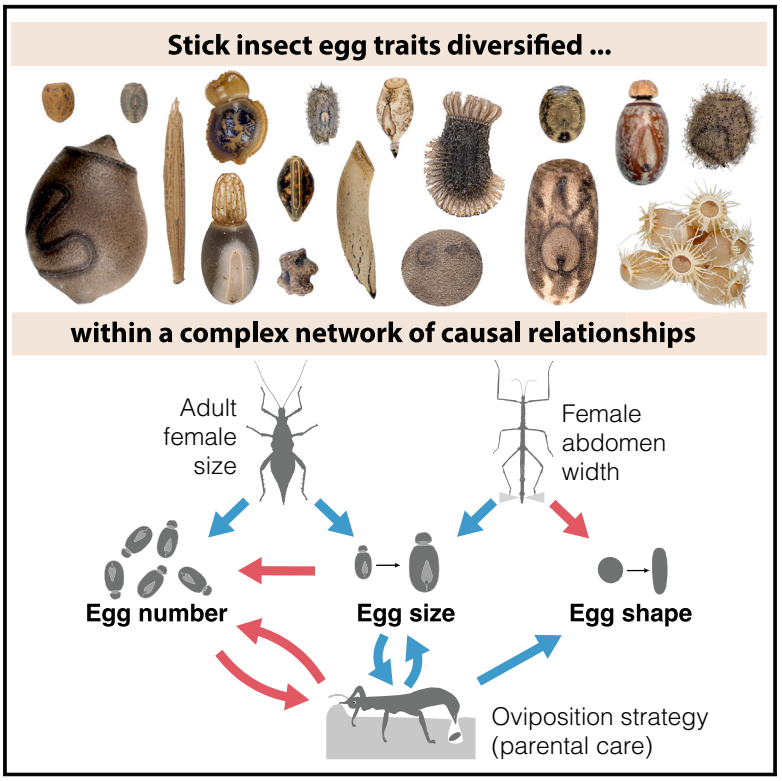

Highlights

- We analyzed patterns of evolution of egg traits from over 200 stick insect species
- Egg traits have diversified within a complex network of causal relationships
- Variation in size is mainly explained by adult size and a trade-off with egg number
- Egg shape evolution is mainly driven by oviposition strategy and female body shape

Authors

Romain P. Boisseau, H. Arthur Woods

Correspondence

romain.boisseau@unil.ch

In brief

Boisseau and Woods investigate factors influencing the evolution of egg morphology in stick insects. Relative egg size appears to be influenced primarily by a trade-off with egg number, while egg shape reflects mechanical constraints arising from the diameter of the female oviduct and oviposition strategy.

Boisseau & Woods, 2024, Current Biology *34*, 2880–2892
July 8, 2024
https://doi.org/10.1016/j.cub.2024.05.042

CellPress

CellPress
OPEN ACCESS

Current Biology

Article

Resource allocation strategies and mechanical constraints drive the diversification of stick and leaf insect eggs

Romain P. Boisseau[1,2,3,4,*] and H. Arthur Woods[1]
[1]Division of Biological Sciences, University of Montana, 32 Campus Drive, Missoula, MT 59812, USA
[2]Department of Ecology and Evolution, University of Lausanne, 1015 Lausanne, Switzerland
[3]X (formerly Twitter): @romainpboisseau
[4]Lead contact
*Correspondence: romain.boisseau@unil.ch
https://doi.org/10.1016/j.cub.2024.05.042

SUMMARY

The diversity of insect eggs is astounding but still largely unexplained. Here, we apply phylogenetic analyses to 208 species of stick and leaf insects, coupled with physiological measurements of metabolic rate and water loss on five species, to evaluate classes of factors that may drive egg morphological diversification: life history constraints, material costs, mechanical constraints, and ecological circumstances. We show support for all three classes, but egg size is primarily influenced by female body size and strongly trades off with egg number. Females that lay relatively fewer but larger eggs, which develop more slowly because of disproportionately low metabolic rates, also tend to bury or glue them in specific locations instead of simply dropping them from the foliage (ancestral state). This form of parental care then directly favors relatively elongated eggs, which may facilitate their placement and allow easier passage through the oviducts in slender species. In addition, flightless females display a higher reproductive output and consequently lay relatively more and larger eggs compared with flight-capable females. Surprisingly, local climatic conditions had only weak effects on egg traits. Overall, our results suggest that morphological diversification of stick insect eggs is driven by a complex web of causal relationships among traits, with dominant effects of resource allocation and oviposition strategies, and of mechanical constraints.

INTRODUCTION

Insect eggs share a common set of characteristics defined by their function: they are propagules—finite packages of resources and information that support embryos as they grow from single cells into complex individuals that hatch into free-living juveniles.[1] Across taxa, eggs are recognizable as such because they share deep homologies. Egg diversity, by contrast, is more difficult to explain. Eggs diverge enormously in size, shape, composition, structure, physiology, and duration of development.[2] What rules structure this diversity? How universal or taxon specific are they? These questions have a long history of study in other taxa, especially birds,[3] reptiles,[4] fish,[5] and marine invertebrates,[6,7] though most studies have focused just on egg size. Below, we briefly outline three non-exclusive classes of hypotheses on the major causes of egg diversification in insects.[8]

Size, life history, and pace of life

An organism's size can predict many other aspects of its life history, including length of development, potential fecundity, metabolic rate, and adult lifespan. In eggs from insect and non-insect taxa, for example, larger adults typically lay larger eggs,[5,9,10] and large eggs typically develop more slowly than small eggs[9,11–16] (but see Church et al.[8]). In addition, like scaling relationships in other taxa and other life stages,[17,18] metabolic rates of eggs scale hypoallometrically with egg mass.[19] Larger adults thus tend to lay larger eggs that develop over longer periods of time, supported by disproportionately low metabolic rates. In addition, egg size may trade off with egg number; females have access to finite resources, and even if they acquire nutrients in adulthood, they face the proximate problem of whether to construct smaller numbers of larger eggs or greater numbers of smaller eggs. Egg size-number trade-offs in insects have been demonstrated both intraspecifically[20–22] and interspecifically.[10,23,24]

Mechanical constraints on egg size and shape

Eggs may face strong geometric constraints on shape as a function of size.[3,8] For example, because eggshell materials are costly (typically rich in protein), females laying more or larger eggs may minimize costs by producing more spherical eggs.[4,10] Conversely, larger eggs may need higher aspect ratios to pass more easily through the reproductive canal during oviposition.[4,10] Larger eggs may also require higher ratios of surface area to volume, allowing them to obtain oxygen at rates high enough to support embryonic metabolism and to minimize diffusion distances to central tissues.[25] In addition, supporting higher metabolic rates may require higher-conductance eggshells, which in turn can lead to higher rates of water loss.[16,26]

CellPress
OPEN ACCESS

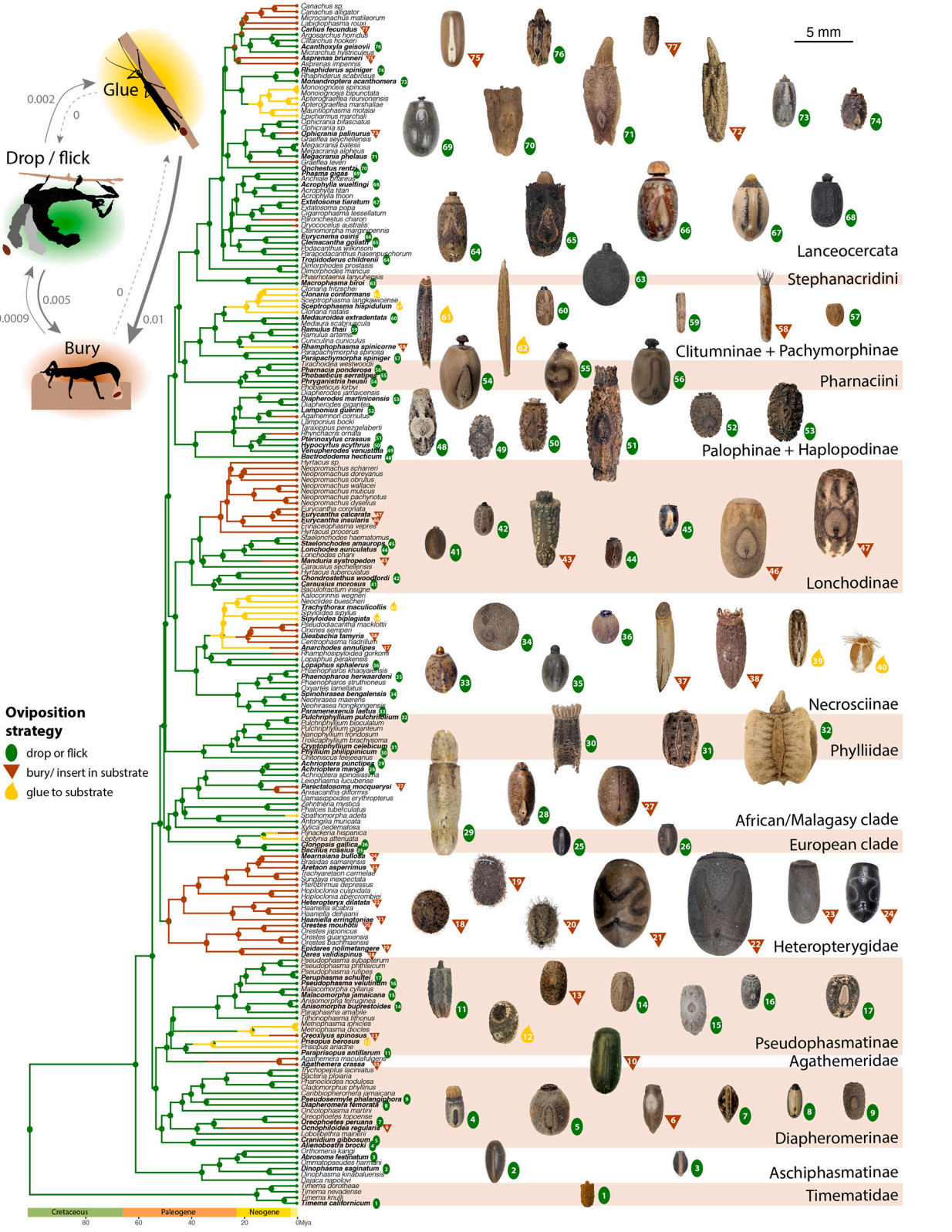

(legend on next page)

Response to ecological circumstances

Egg traits may evolve in response to local suites of ecological conditions, including (1) patterns of predation in relation to size, placement, or camouflage of the eggs, or as functions of the mechanical and chemical defenses that they deploy[27,28]; (2) whether females are flight-capable or flightless[3]; and (3) local environmental conditions in their microsites, including whether eggs are aquatic or aerial.[8]

Church and Donoughe et al.[8] recently examined a subset of these possibilities using data on egg and adult traits derived from over 6,700 species in 526 families distributed across all extant orders, although not all traits were available for all species. Using phylogenetic analyses, they reached three main conclusions. First, geometric constraints on egg diversification were detectable but weak; larger eggs tended to have higher aspect ratios. Second, larger females tended to lay larger eggs, but contrary to other studies, those eggs did not have systematically longer developmental periods. Third, the most important drivers of changes in egg size and shape were the ecological circumstances of oviposition. In particular, evolutionary shifts from aerial oviposition (onto exposed surfaces) to aqueous oviposition (into water or body fluids) led to systematic reductions in egg size and changes in shape.

Because of the large dataset used, the analyses of Church and Donoughe et al.[8] are uniquely comprehensive and powerful. Nevertheless, some conclusions—e.g., that larger eggs do not take longer to develop—are surprising and may reflect that some analyses were constrained by lack of data to a relatively small number of species distributed across multiple major clades. Such a situation may increase the probability that patterns in focal traits, even if present, are obscured by other evolved differences among clades (i.e., orders). A complementary approach would be to focus on more closely related groups with extensive sampling of species from across the group phylogeny.[2,29] Here we present such an analysis for stick and leaf insects (order Phasmatodea), which appear to have originated in the early Cretaceous and diversified extensively following the K-T boundary[30,31] (but see Tihelka et al.[32]). Worldwide, there are more than 3,500 described species,[33] for which we have compiled data on morphological and developmental traits of eggs and adults on 208 species from approximately 27% of the ~520 described genera.

As masters of crypsis and masquerade, stick and leaf insects show remarkably diverse body morphologies, ranging from elongated stick-like silhouettes to robust, stocky forms.[34] They also produce remarkably diverse eggs, which span wide ranges in size, shape, and structure.[35] Eggs of some Heteropteryginae, for example, are among the largest produced by any insect, reaching 300 mg and 12 mm in length in *Haaniella echinata*.[36] By contrast, eggs of *Spinoparapachymorpha spinosa* (Clitumninae) are only 2 mg and 1.6 mm in length.[37]

In Euphasmatodea, the evolution of a hardened egg chorion is a key innovation and may have contributed to the group's extreme diversification[35] by opening multiple routes of unusual dispersal.[31,38] Hard shells and their associated structures can withstand hazardous falls from the forest canopy, float for extended periods of time on seawater (hydrochory),[39] bear ant-attractive capitula (analogous to plants' eliasomes, myrmecochory),[40,41] and survive passage through the guts of birds (endozoochory).[42,43] Accordingly, female phasmids employ a variety of egg-laying strategies, including passively dropping or actively flicking eggs to the forest floor, burying them in soil or other soft substrates, and gluing them to plant surfaces individually, in groups, or inside complex ootheca.[31,44] Since the late 1800s,[45–47] biologists have suggested that the morphological resemblance of phasmid eggs to seeds is a form of mimicry or masquerade. Although this resemblance is indeed impressive, its ecological and evolutionary significance is still largely unknown.[38]

Owing to their extreme diversity, relatively large size, and ease of breeding in captivity, stick insects are commonly kept as pets by amateur breeders or in classrooms, which has facilitated the compilation of a large dataset on egg size, shape, and physiology.[37,48,49] We leverage this comparative dataset in a phylogenetic context, along with additional data on rates of metabolism and water loss by eggs of five of the species, to evaluate the relative importance of the diversifying factors proposed above. Overall, signatures of many factors appeared in patterns of egg diversification. Nevertheless, causal relationships (derived from phylogenetic path analyses) between these factors suggested that egg size was mostly affected by resource allocation strategies and trade-offs and by oviposition strategy, while egg shape was mostly influenced by mechanical constraints.

RESULTS

Phylogenetic analysis of transitions in oviposition style

Our reconstructions unambiguously indicated that the ancestor lineages of Phasmatodea and Euphasmatodea dropped or flicked their eggs to the ground (Figure 1). The associated transition matrix identified asymmetric transition rates between oviposition modes and suggested that transitions from dropping/flicking to burying (≥16 times) or gluing (≥7 times) and from gluing to burying (≥3 times) were most frequent. Only one reverse transition back to dropping/flicking from burying was recovered (equivocally) in the New Zealand/New Caledonia clade (Lanceocercata; Figure 1), highlighting that reverse transitions from more derived styles were very unlikely. Morphologically and ecologically diverse clades that colonized diverse habitats often exhibited more diverse oviposition styles with multiple transitions.[34]

Size, life history, and pace of life

Across phasmids, larger females laid more and larger eggs (Figures 2A and 2B; Table S2). After accounting for adult female body volume, we found a negative correlation (a trade-off) between lifetime egg number (fecundity) and egg volume (Figure 2C). Oviposition mode significantly affected the size-number trade-offs. Females burying or gluing eggs in specific locations,

Figure 1. Egg morphological diversity and ancestral state reconstruction of oviposition mode in Phasmatodea

The ancestral state reconstruction used stochastic character mapping and a transition matrix (inset) estimated by maximum likelihood. Scaled egg pictures in dorsal view correspond to the species listed in Table S1. Dropped or flicked eggs are represented by a green oval, buried eggs by a brown triangle, and glued eggs by a yellow droplet.

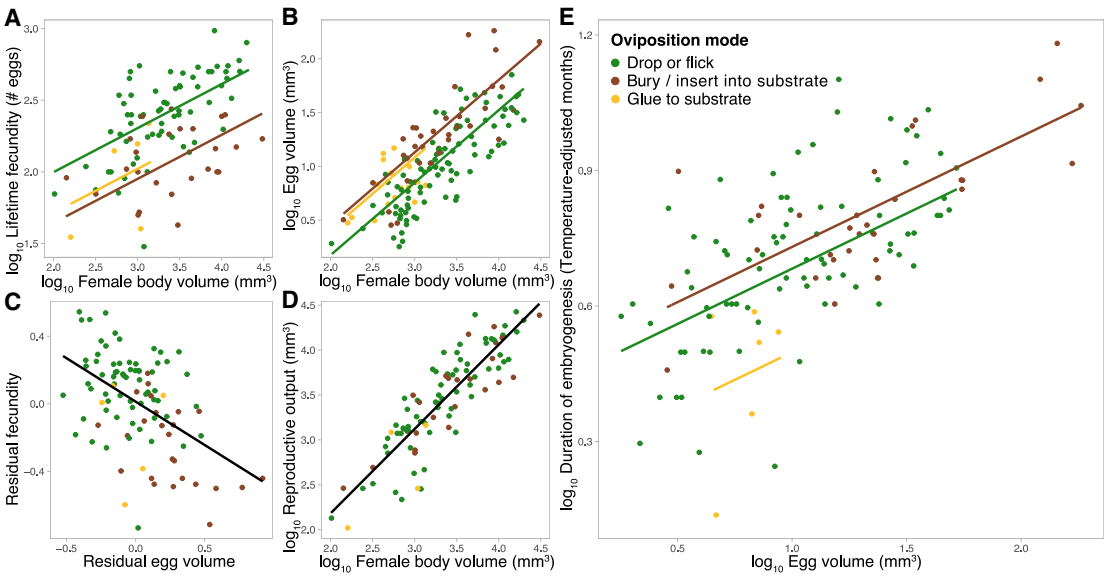

Figure 2. Life history predictors of egg size

(A) Lifetime fecundity compared with adult female body volume.

(B) Egg volume compared with adult female body volume.

(C) Relationship between relative lifetime fecundity and relative egg volume after accounting for female body volume.

(D) Lifetime reproductive output (fecundity × egg volume) as a function of female body volume.

(E) Duration of embryogenesis (corrected for temperature), from egg laying to hatching, compared with egg volume. Colors represent different oviposition modes (see legend). Phylogenetic least-square regressions are represented and correspond to the analyses in Table S2.

i.e., that invest more in parental care, laid fewer but larger eggs relative to females that drop or flick their eggs. Overall, lifetime reproductive output (lifetime fecundity × egg volume) was strongly correlated with adult female volume but did not differ between oviposition modes (Figure 2D). Larger eggs developed slower than smaller eggs, and for a given volume, glued eggs developed faster than buried or dropped eggs (Figure 2E).

Mechanical constraints on egg size and shape

A phylogenetic principal component analysis revealed that most variation in egg capsule shape reflected variation in aspect ratio: PC1 (66% of total variation) reflected variation in elongation, and PC2 (21% of total variation) separated dorso-ventrally from laterally flattened eggs (Figures 3A and S1B–S1D). Most phasmid eggs were clustered in the center of the egg morphospace, exhibiting a generic barrel shape (Figure 3A). By contrast, other species had elongated or flattened lentil-shaped capsules.

Egg width was positively correlated with length in dropped and buried eggs, but not in glued eggs (Figure 3B; Table S3). The scaling relationship between width and length was significantly hypoallometric in dropped eggs (β = 0.78 ± 0.07, 95% CI = [0.64; 0.92], isometric slope = 1) but did not differ from isometry in buried eggs (β = 1.03 ± 0.18, 95% CI = [0.68; 1.39]). Buried eggs were relatively more elongated than dropped eggs (Figure 3B), while glued eggs ranged from the most elongated to more spherical, notably in species where females glue eggs in batches (Figure 3A). This morphological diversity suggests a strong influence of substrate properties on which eggs are glued (bark, grass, leaves) and laying strategy (eggs laid singly or in batches).

Overall, surface area scaled isometrically with egg volume (β = 0.65 ± 0.01, 95% CI = [0.633; 0.674], isometric slope = 0.667), and this relationship was not affected by oviposition mode (Figure 3C).

Egg width scaled hypoallometrically with the width of the female's ninth tergite, where the opening of the oviduct is located (the putative maximum egg width that can pass through the oviduct) (Figure 3D; β = 0.68 ± 0.04, 95% CI = [0.60; 0.77], isometric slope = 1). The width of almost all eggs was smaller than that of the ninth tergite (Figure 3D). Glued and buried eggs were relatively wider and sometimes slightly wider than the ninth tergite, suggesting potential dilatation of the oviduct (Figure 3D). Residual egg width after accounting for length was positively correlated with residual female ninth tergite width, after accounting for female volume, in species that bury or glue their eggs but not in species that drop or flick them (Figure 3E). Thus, females with relatively narrower abdomens lay relatively more elongated eggs, but this relationship held only for species that bury or glue their eggs, which tend to be larger (Figure 2B) and closer to the width limit imposed by the oviduct opening (Figure 3D). This suggests that, in species with more derived oviposition modes and larger eggs, egg width is constrained by the diameter of the female oviduct opening, or vice versa.

Response to ecological circumstances

After accounting for adult female volume, lifetime fecundity, and oviposition mode, we found significant effects of female flight capacity and climate PC1 on egg volume (Table 1). Flight-capable females and females living in more temperate and seasonal regions (reflected by climate PC1) laid relatively smaller eggs.

After accounting for egg volume, egg surface area was not significantly affected by any of our ecological predictors. Therefore, species experiencing drier conditions, either seasonally

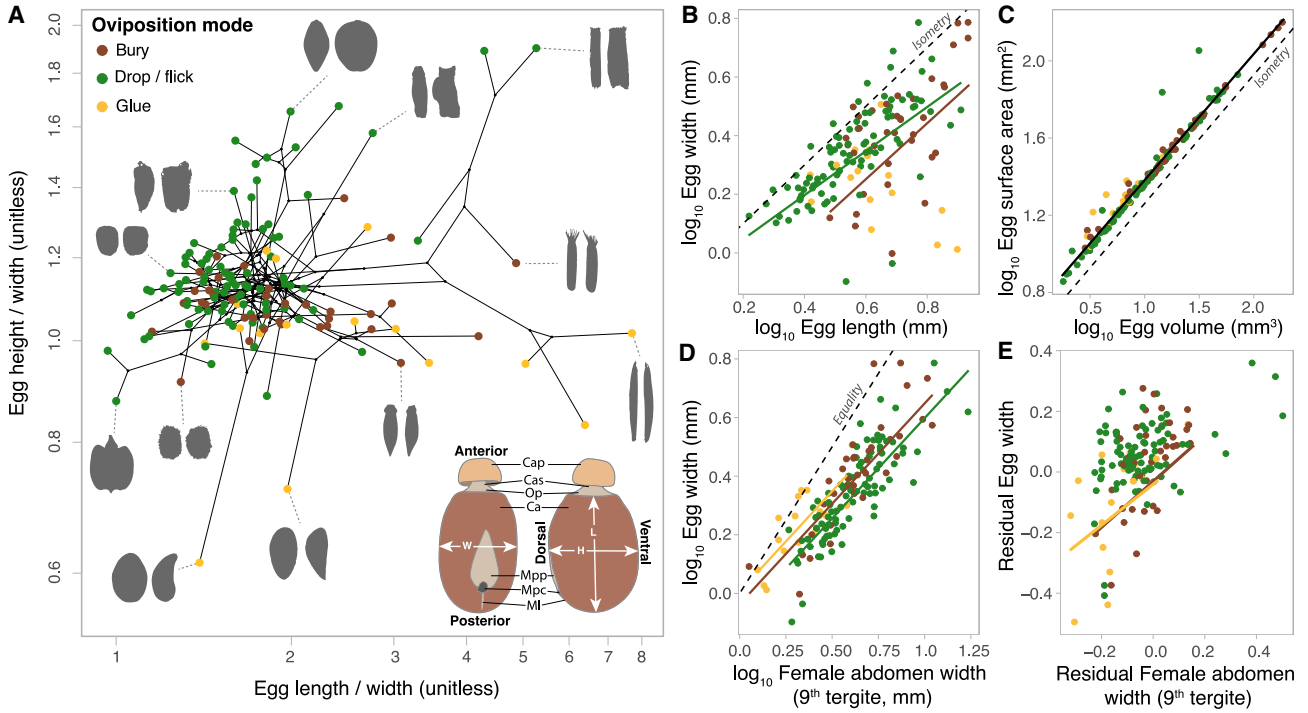

Figure 3. Egg shape and allometric scaling

(A) Phasmid egg morphospace showing egg length over width and height over width. These aspect ratios explain most of the variation in egg shape (Figure S1). Black lines between points represent underlying phylogenetic relationships. Egg silhouettes are represented in dorsal (left) and side (right) view. Bottom right inset shows the drawing of a phasmid egg (*Eurycnema osiris*). Cap, capitulum; Cas, capitulum stalk; Op, operculum; Ca, egg capsule; Mpp, micropylar plate; Mpc, micropylar cup; Ml, median line; L, egg length; W, egg width; H, egg height.

(B) Egg width as a function of egg length.

(C) Egg surface area as a function of egg volume.

(D) Egg width as a function of the width of the adult female ninth tergite (i.e., where the egg is released).

(E) Residual egg width (residuals from the phylogenetic generalized least-square [PGLS] regression between egg width and egg length) compared with residual width of female ninth tergite (residuals from the PGLS regression between the width of ninth tergite and adult female body volume).

Phylogenetic least-square regressions are shown in (B)–(E) and correspond to the analyses in Table S3. Colors correspond to oviposition mode (see legend in A). Dashed lines represent isometric slopes (arbitrary intercept) in (B) and (C) or the equality line in (D).

(high climate PC2) or constantly (low climate PC1), do not seem to minimize egg surface-to-volume ratio to limit water loss.

After accounting for egg length, relative egg width (aspect ratio) was significantly affected by oviposition mode and climate PC1. Glued and buried eggs were more elongated than dropped eggs, and eggs of species found in drier and more temperate and seasonal regions were slightly more elongated (Table 1).

Total female reproductive output was significantly affected by female flight capacity and climate PC1, even after accounting for female body volume. Flightless females were able to invest relatively more in egg production than were flight-capable ones. This suggests either a physiological cost of the flight apparatus or of carrying more and/or larger eggs, and potentially explains why even after accounting for relative fecundity, flightless females lay relatively larger eggs. Similarly, females in regions with higher net primary productivity (which may provide more food) invested relatively more in egg production, also suggesting that females in temperate and less productive regions may be more resource limited. This may also explain why tropical females lay relatively larger eggs even after accounting for relative fecundity. However, we note that our fecundity data were mostly obtained from breeding cultures, in which insects are fed *ad libitum*. Alternatively, differences in total reproductive investment may reflect reduced adult life spans in seasonal regions with short periods of favorable conditions.

Finally, after accounting for variation in egg volume, duration of embryogenesis was affected only by oviposition mode, with glued eggs developing relatively faster than buried and dropped eggs (Tables 1 and S2). The other ecological variables had no significant effects.

Phylogenetic path analyses

Phylogenetic path analyses were used to infer possible causal relationships among traits (Figure 4). This analysis revealed that variation in egg size has been driven by many variables related to all three hypothesis categories: tropical climates, larger body size, relatively wider abdomens, parental care, and flight loss in females all favored the evolution of larger eggs. Conversely, variation in egg size has driven variation in various life history and behavioral traits: larger eggs reduce female fecundity (total egg number), lengthen embryonic development, facilitate range shifts toward more tropical climates, and drive the evolution of parental care (oviposition in specific locations). Parental care and egg size and number appeared mutually

Table 1. Effect of ecological variables on egg size and shape

Predictor	λ	$F_{df1,df2}$	*p*	Effect size ± standard error (cont.) or post hoc pairwise tests (Holm) (cat.)
Response variable: log_{10} egg volume (*n* species = 96)				
log_{10} female body volume[a]	0.44	$F_{1,88} = 176.6$	<0.0001	0.66 ± 0.06
log_{10} lifetime fecundity[a]		$F_{1,88} = 30.36$	<0.0001	−0.29 ± 0.09
oviposition mode[a]		$F_{2,88} = 6.61$	0.002	drop − bury = −0.15 ± 0.07, $p = 0.07$; drop − glue = −0.08 ± 0.12, $p = 0.98$; bury − glue = 0.07 ± 0.11, $p = 0.98$
adult female flight capacity[a]		$F_{1,88} = 6.84$	0.01	flying − flightless = −0.21 ± 0.08, $p = 0.009$
climate PC1 (∼net primary production, annual temperature, and precipitation)[a]		$F_{1,88} = 10.46$	0.002	0.09 ± 0.02
climate PC2 (∼precipitation seasonality)		$F_{1,88} = 1.63$	0.20	−0.03 ± 0.02
Response variable: log_{10} egg surface area (*n* species = 96)				
log_{10} egg volume[a]	0.72	$F_{1,88} = 1,802.1$	<0.0001	0.65 ± 0.02
log_{10} lifetime fecundity		$F_{1,88} = 0.01$	0.91	0.009 ± 0.02
oviposition mode		$F_{2,88} = 0.34$	0.71	drop − bury = −0.010 ± 0.02, $p = 1$; drop − glue = −0.016 ± 0.03, $p = 1$; bury − glue = −0.006 ± 0.03, $p = 1$
adult female flight capacity		$F_{1,88} = 0.04$	0.83	flying − flightless = 0.005 ± 0.02, $p = 0.82$
climate PC1 (∼net primary production, annual temperature, and precipitation)		$F_{1,88} = 0.75$	0.39	0.007 ± 0.007
climate PC2 (∼precipitation seasonality)		$F_{1,88} = 1.30$	0.26	−0.007 ± 0.006
Response variable: log_{10} egg width (*n* species = 143)				
log_{10} egg length[a]	0.98	$F_{1,136} = 104.9$	<0.0001	0.65 ± 0.07
oviposition mode[a]		$F_{2,136} = 6.96$	0.001	drop − bury = 0.08 ± 0.03, $p = 0.009$; drop − glue = 0.11 ± 0.04, $p = 0.009$; bury − glue = 0.03 ± 0.04, $p = 0.39$
adult female flight capacity		$F_{1,136} = 1.39$	0.24	flying − flightless = −0.03 ± 0.03, $p = 0.23$
climate PC1 (∼net primary production, annual temperature, and precipitation)[a]		$F_{1,136} = 7.65$	0.006	0.03 ± 0.01
climate PC2 (∼precipitation seasonality)		$F_{1,136} = 2.97$	0.09	−0.01 ± 0.008
Response variable: log_{10} reproductive output (egg number × volume) (*n* species = 96)				
log_{10} female body volume[a]	0.19	$F_{1,89} = 295.6$	<0.0001	0.86 ± 0.06
oviposition mode		$F_{2,89} = 2.59$	0.08	drop − bury = 0.10 ± 0.07, $p = 0.45$; drop − glue = 0.15 ± 0.14, $p = 0.59$; bury − glue = 0.05 ± 0.15, $p = 0.73$
adult female flight capacity[a]		$F_{1,89} = 4.13$	0.045	flying − flightless = −0.22 ± 0.10, $p = 0.03$
climate PC1 (∼net primary production, annual temperature, and precipitation)[a]		$F_{1,89} = 9.32$	0.003	0.09 ± 0.03
climate PC2 (∼precipitation seasonality)		$F_{1,89} = 0.04$	0.84	0.006 ± 0.03
Response variable: Duration of embryogenesis (temperature corrected) (*n* species = 121)				
log_{10} egg volume[a]	0.35	$F_{1,111} = 68.4$	<0.0001	0.26 ± 0.04
oviposition mode[a]		$F_{2,111} = 6.69$	0.002	drop − bury = −0.056 ± 0.03, $p = 0.11$; drop − glue = 0.20 ± 0.07, $p = 0.005$; bury − glue = 0.26 ± 0.07, $p = 0.0008$
adult female flight capacity		$F_{1,111} = 0.33$	0.56	flying − flightless = 0.03 ± 0.05, $p = 0.57$
climate PC1 (∼net primary production, annual temperature, and precipitation)		$F_{1,111} = 0.67$	0.41	−0.013 ± 0.015
climate PC2 (∼precipitation seasonality)		$F_{1,111} = 1.35$	0.25	0.015 ± 0.013

The table presents the results of phylogenetic generalized least-square (PGLS) models. The most likely value of Pagel's lambda (phylogenetic signal) is presented along with type-I (sequential) ANOVA outputs and either estimated effect sizes or post hoc pairwise comparisons between estimated marginal means using the Holm method to account for multiple testing, respectively, for continuous or categorical explanatory variables.
[a]Significant effect ($p < 0.05$)

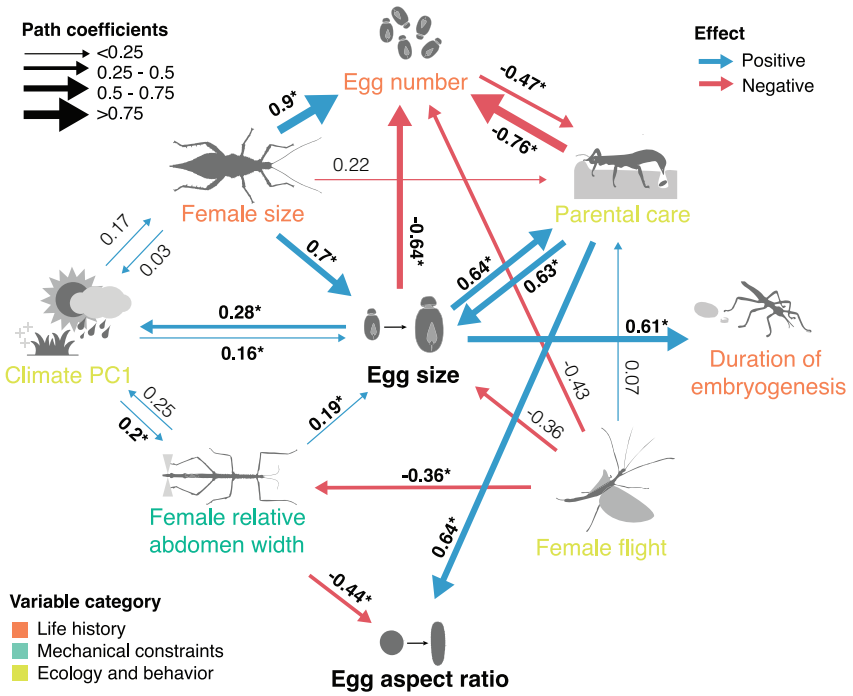

Figure 4. Averaged best-fitting path models (ΔCICc < 2)

Arrows show the direction of the path. Their color and width represent direction and size of regression coefficient (adjacent to arrows). Coefficients deviating significantly from 0 are written in bold with an asterisk.

reinforcing: females laying fewer, larger eggs are more likely to evolve parental care, while parental care also seemed to favor the evolution of fewer, larger eggs. Similarly, more temperate climates (lower climate PC1) appeared to favor smaller eggs and smaller, narrower females, while smaller eggs and smaller, narrower females likely favored range expansion into temperate regions. In parallel, egg shape has also evolved in response to changes in several other traits: smaller and thinner females produce more elongated eggs, likely highlighting mechanical constraints for the egg to pass through the reproductive canal. Females burying or gluing their eggs produce more elongated eggs, likely facilitating their insertion into substrates or adhesion to surfaces.

Egg metabolic rate, energy use, and water loss

The five sampled species differed extensively in egg size and duration of embryogenesis, from 4.07 ± 0.07 mg and 98 ± 0.9 days in *Medauroidea extradentata* to 155.9 ± 2.4 mg and 341 ± 6.8 days in *Heteropteryx dilatata*. Metabolic rate increased exponentially during development in all five species (Figure 5A). Mid-development, mean, and maximum metabolic rates scaled hypoallometrically across species (respectively $\beta = 0.70 \pm 0.16$, 95% CI: [0.36; 0.98], $\beta = 0.78 \pm 0.10$, [0.58; 0.97], $\beta = 0.76$ [0.65; 0.87]; Figures 5B, S2A, and S2B; Table S4), indicating that larger eggs had relatively lower metabolic rates than smaller eggs. Estimated cumulative CO_2 produced during embryogenesis scaled isometrically (Figure 5C; Table S4), suggesting that eggs use approximately the same proportion of their total energy regardless of size.

At 100% relative humidity, in *E. calcarata* ($\beta = -0.01 \pm 0.01$ mg.day^{-1}, Wald χ^2 test: $\chi^2 = 1.03$, df = 1, $p = 0.3$) and in *M. extradentata* ($\beta = -0.0008 \pm 0.0007$ mg.day^{-1}, $\chi^2 = 1.54$, df = 1, $p = 0.21$), egg mass did not significantly decrease over time. By contrast, for *H. dilatata* ($\beta = -0.03 \pm 0.002$ mg.day^{-1}, $\chi^2 = 176.8$, df = 1, $p < 0.0001$), *P. philippinicum* ($\beta = -0.002 \pm 0.0006$ mg.day^{-1}, $\chi^2 = 9.38$, df = 1, $p = 0.002$), and *E. tiaratum* ($\beta = -0.005 \pm 0.0007$ mg.day^{-1}, $\chi^2 = 43.9$, df = 1, $p < 0.0001$), we found a significant decrease of mass over time. This decrease may stem from the loss of organic matter through catabolism or water loss during flow-through respirometry. However, mass loss rates estimated through the same method for eggs held at 75% relative humidity showed much higher values (*H. dilatata*, $\beta = -0.11 \pm 0.002$ mg.day^{-1}; *P. philippinicum*, $\beta = -0.008 \pm 0.001$ mg.day^{-1}; *E. tiaratum*, $\beta = -0.013 \pm 0.001$ mg.day^{-1}), suggesting that most of the mass lost by eggs at 75% relative humidity was water. In all five species, eggs lost water at a constant rate during embryogenesis at 75% relative humidity (Figures 5D and S2C), and this rate increased hypoallometrically with egg mass after accounting for oviposition mode (Figure 5E). The recovered scaling exponent (0.29 ± 0.07, [0.15; 0.43]) when the model included a term for oviposition mode (burying versus dropping/flicking) was significantly lower than the expected scaling exponent of egg surface area with egg mass (0.66), suggesting that larger eggs have reduced chorion permeability, possibly from increased thickness or changes in layer properties.[50] The unexpectedly low slope, however, may also have arisen from including the oviposition term, which accounted for much of the variance; without that term, the recovered slope was 0.65, closer to the slope of surface area. Given the small number of species for which we have detailed physiological data ($n = 5$), it is not possible to resolve which model is better, and we call for more work on a broader range of species. Regardless, water loss rate was relatively higher in the two largest species, which bury their eggs. Finally, we found a strong isometric relationship between egg water content and egg mass (Figure 5F), suggesting that small and large eggs contain the same proportion of water (49% ± 0.01%).

DISCUSSION

Using a single mesodiverse clade of insects—the stick and leaf insects (order Phasmatodea)—we assessed hypothesized drivers of egg diversification by combining phylogenetic analyses with physiological measurements of metabolism and water loss. Together, the data suggest that morphological diversification is driven by a complex suite of factors, including female resource allocation strategies, constraints

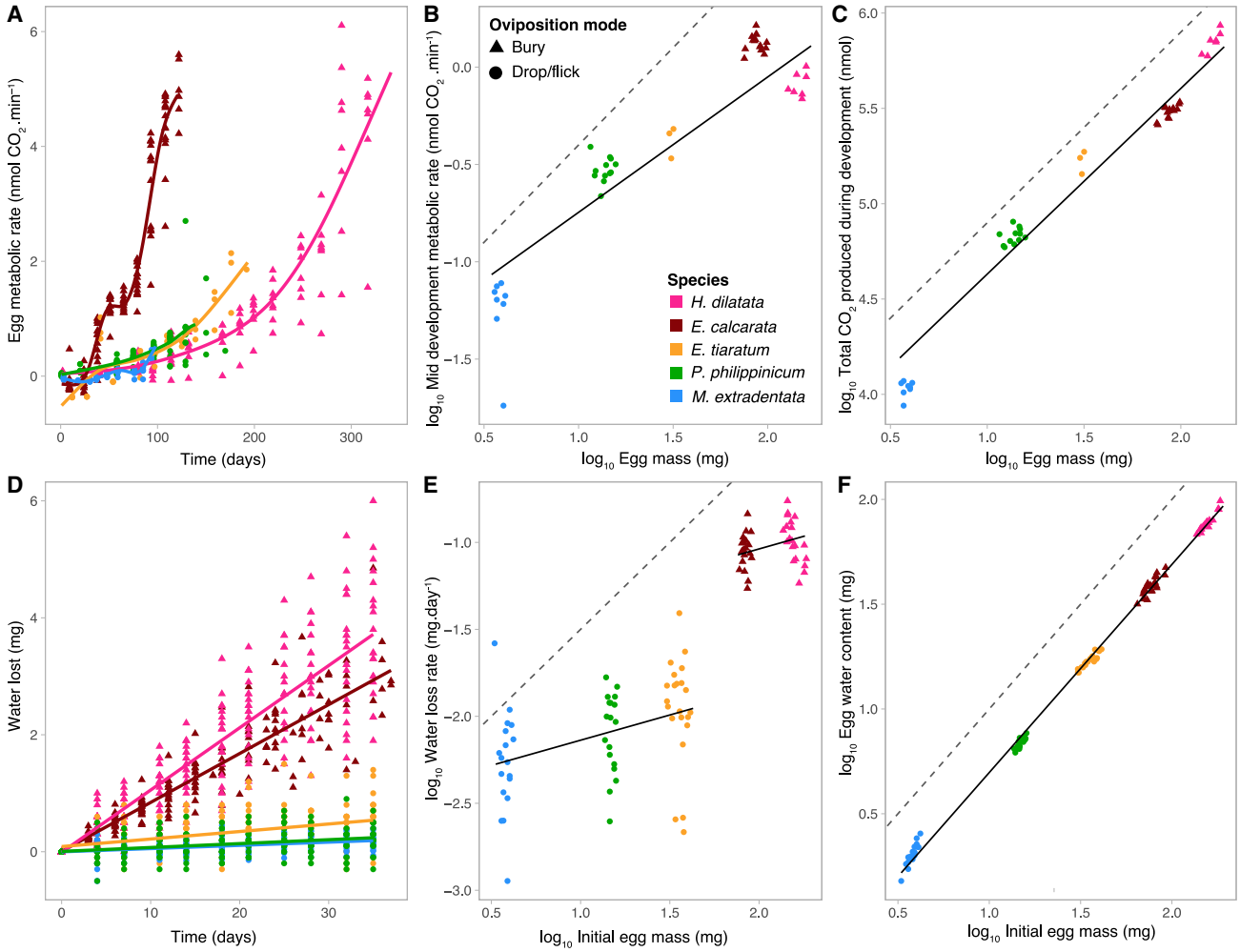

Figure 5. Allometry of egg energy use and water loss

(A) Egg metabolic rate as a function of time (until hatching). Lines depict smoothing generalized additive models for each species.

(B) Estimated mid-embryogenesis metabolic rate compared with egg mass.

(C) Estimated total CO_2 produced during embryogenesis as a function of egg mass.

(D) Cumulative egg water loss as a function of time (until hatching). Lines depict linear regressions for each species.

(E) Water loss rate compared with initial egg mass (right after oviposition).

(F) Initial egg water content as a function of initial mass.

Colors represent the five different species, and shapes represent oviposition modes (see legend in B). Dashed lines represent isometry (arbitrary intercept). Solid black lines represent linear mixed-effects regressions (see Table S4 for details).

See also Figure S2.

arising from eggs interacting mechanically with functions of the female body, the effects of female oviposition and locomotor (flight) behavior, and to a lesser extent, the influences of climate in which lineages have evolved.

In our analyses, variation in egg size was driven mainly by female resource allocation strategies and trade-offs. Larger females lay more, larger eggs, but egg size limits egg number (Figures 2A–2C and 4), providing strong evidence of egg size-number trade-offs, consistent with previous studies on insects.[23,24] The total reproductive investment of females (total lifetime mass of eggs laid) was tightly related to female size (Figure 2D). This highlights that females have access to limited resources for reproduction, which they may allocate among fewer larger or more smaller eggs. Interestingly, we found a negative effect of flight capacity on egg size and number (Figure 4; Table 1): flightless females had higher lifetime reproductive investment, laying both more and larger eggs compared with flight-capable ones. This pattern suggests that physiological costs of wings and associated flight muscles may trade off with reproductive output.[51] Alternatively, large eggs may impair the flight performance by increasing wing loading.[52] Stick and leaf insects are ideally suited to address how flight affects resource allocation strategies and egg diversification, as they have undergone numerous shifts between winged and wingless forms.[53–55] In accordance with Church and Donoughe et al.,[8] we found no effect of flight capacity on egg shape, in contrast with a study of birds.[3]

Larger eggs also consistently required longer periods of time to develop, in striking contrast to the data reported by Church and Donoughe et al.[8] The difference likely reflects the phylogenetic scope of analysis.[29] Church and Donoughe et al.[8] used data on 66 genera distributed across seven major insect orders (hemi- and holometabolous), such that order-specific differences may have obscured direct effects of egg size, if any, on duration of development. By contrast, our study, which analyzed 136 species in a single order, finds strong evidence that larger eggs require longer developmental periods. This result is consistent with other reports on insects[9,12,13] and vertebrates.[14,15,56]

Consistent with our observation that large eggs require longer developmental periods, egg size also had systematic effects on egg metabolism and water loss: both rates scaled hypoallometrically, such that large eggs had disproportionately low rates. Although the confidence intervals are wide due to the low number of species used (five), values of the metabolic scaling coefficient (β = 0.70, 95% CI: [0.36; 0.98] for mid-development metabolic rate; β = 0.78 [0.58; 0.97] for mean metabolic rate) lie in the range expected from other metabolic scaling studies (insect eggs, β = 0.92 [0.86; 0.98][19]; non-avian reptile eggs, β = 0.82 [0.77; 0.87][57]; avian eggs, β = 0.714 ± 0.09 [SE][58,59]; ectotherm eggs, β = 0.66 [0.65; 0.80][60]).

The emerging picture is of larger eggs generally having longer developmental durations (β = 0.24) supported by lower mass-specific metabolic rates (mean rate: β = 0.78). Jointly, these scaling effects indicate that total energy use should be approximately isometric (β = 0.24 + 0.78 = 1.02), a conclusion supported by our estimates of total energy use (β = 0.97; Figure 5C). There is scope, however, for additional covariation in metabolic rates and developmental duration beyond the effects of size. For example, the largest eggs in our experiment, *E. calcarata* (84.2 ± 0.8 mg) and *H. dilatata* (155.9 ± 2.4 mg), had relatively similar metabolic rates at the temporal midpoint of development (Figure 5B). However, *E. calcarata* eggs develop much faster (121 ± 2 versus 335 ± 5 days), supported by a much more rapid increase in metabolism across development (Figure 4A). In insects, long development times are often associated with a period of diapause.[61] Remarkably, *H. dilatata* eggs did not exhibit diapause despite an exceptionally long embryogenesis, as they showed a continuous increase in metabolic rate.[61]

Like total CO_2 production, total egg water content also scaled isometrically, as it does in bird eggs[62] (β = 0.97; 95% CI 0.95–0.99) and butterfly eggs[63] (β = 1.09; 95% CI 1.01–1.18). Collectively, these observations suggest that egg size, developmental duration, rates of energy and water expenditure, and total energy reserves are all tightly correlated.[56] This outcome likely reflects the division of eggs into finite packets of energy and materials that exchange only water, carbon dioxide, and oxygen with their surroundings. Here too, however, it appears that ecological circumstances lead to altered relationships. For example, rates of water loss in the species that bury their eggs (*H. dilatata*, *E. calcarata*; Figure 5E) were higher for their size than rates from the other species, which drop or flick their eggs. This likely reflects that soils often have very high relative humidities[64,65] but are also prone to hypoxia when wet, especially in warm, rich soils.[66] In response, egg-burying species may evolve higher-conductance eggshells to take up oxygen better from hypoxic air spaces underground while incurring little additional risk of desiccation.[26]

A major factor influencing the variation in relative egg size and number was female oviposition strategy. Female phasmids either drop or flick their eggs (the ancestral state; Figure 1) or place them in specific locations, typically gluing or burying them. Burying likely benefits embryos by sheltering them from egg predators, parasitoids, and risk of desiccation. By contrast, offspring of glued eggs hatch directly onto their host, saving time and effort associated with finding a suitable host and climbing it (see Brock and Hasenpusch[48]). Larger and fewer eggs appeared to favor placement in specific locations (Figures 2A–2C and 4), implying greater parental investment per offspring associated with the greater time investment and predator exposure during oviposition. In parallel, the specific placement of eggs also appeared to favor fewer, larger eggs, suggesting a feedback loop of mutual causality (Figure 4). Similar positive relationships between parental care and egg size have also been found in other ectotherms including fishes[67] and frogs[68] and in theoretical studies[69] (but see Gilbert and Manica[70]). In addition, glued (but not buried) eggs evolved significantly shorter developmental durations for their size (Figure 2E). Glued eggs may be more vulnerable to egg predators and parasitoids, which likely select for rapid development.[71]

Gluing and burying favored the evolution of more elongated eggs (Figure 4). This effect may reflect one or more of several pressures: ease of oviposition, camouflage,[28] enhanced oxygen access,[25,72] or contact surface area for adhesion.[73,74] Phasmids repeatedly evolved very elongated female body shapes, likely as a result of twig mimicry (masquerade).[34] Consequently, the resulting narrow abdominal shapes appear to have favored smaller, more elongated eggs (Figure 4). Females of species that glue or bury eggs produce relatively larger eggs and therefore may be particularly affected by these constraints as their egg widths can approach or exceed the widths of abdominal segments through which they pass (Figures 3D and 3E). Similarly, in birds, egg shape appears largely determined by anatomical constraints imposed by oviduct and pelvis width.[3,75]

One surprising outcome of our analyses was the minimal predictive effects of climate, even though the species studied are distributed across a range of tropical and temperate habitats[76–78] (Figure S3). *A priori*, one might expect that eggs in habitats with low annual precipitation would be larger and rounder to maximize water retention via reduced surface-to-volume ratios; that eggs in more seasonal and potentially unfavorable environments would be larger to favor hatchling survival and performance[79]; or that eggs in less productive environments would be smaller because of a reduced reproductive investment.[80] Indeed, we found evidence that females from temperate and drier areas associated with lower net primary productivity tended to be smaller and to lay slightly smaller, rounder eggs, even after accounting for female size and fecundity (Figure 4). Thus, we show that these females invest less in egg production compared with tropical females. Our path analysis also suggested that female morphology and climate variables (i.e., species range) co-evolved, with smaller, thinner females laying smaller eggs, facilitating the colonization of temperate regions. Overall, however, effect sizes of the climate variables (collapsed into principal components) were small compared with effect sizes of other predictors (Figure 4; Table 1). This outcome likely reflects that egg experience is poorly captured by the large-scale gridded climate data that we used (bin size 4.6 km on a side). Eggs experience

soil and leaf microclimates that may differ strongly from conditions characterizing macroclimatic grid cells.[81,82]

Overall, our results on Phasmatodea align with the broad findings of Church and Donoughe et al.[8] in identifying a strong association between oviposition ecology and egg size and shape. In their study, ''oviposition ecology'' referred to whether eggs were laid in aerial environments or in aquatic environments, which characterizes insects laying eggs in freshwater and parasitoids laying eggs in tissues of other animals. Eggs laid in aquatic environments were smaller and more elongated. We were unable to test the consequences of transitions between aerial and aquatic oviposition, as no phasmids oviposit in water or are parasitoids. Our data on phasmids further suggested that oviposition mode co-evolves with egg size, which in turn influences egg shape. These results suggest that renewed attention should be directed toward understanding how ovipositing females experience interactions between eggs and their substrates and the physical and biotic experiences of eggs in their microsites.

The staggering diversity of insect eggs is obvious, but the major processes that explain it have been obscure. Recent studies leveraging larger datasets, including this one, are starting to reveal drivers and consequences of diversity. Variation in egg size appears to be driven mainly by variation in oviposition mode, female resource allocation strategies, and trade-offs, while egg shape appears to be influenced primarily by mechanical constraints imposed by the female body morphology and by oviposition mode and substrate. However, variation in eggshell morphology and structure remains largely unexplained,[35] despite its key roles in mediating gas and water exchange and mechanical protection. As suggested by our data on a few species, different microclimates (below- versus aboveground) are likely to affect physiological properties of the eggshell (e.g., water permeability). Moving forward, it will be important to integrate data on egg size, shape, and eggshell morphology with ecological, life history, functional, and physiological data on a large set of species. Because they have evolved some of the most diverse and elaborate eggshell structures,[31,35,74] stick insects appear ideally suited for understanding the coevolution of ecology and egg morphology.

STAR★METHODS

Detailed methods are provided in the online version of this paper and include the following:

- KEY RESOURCES TABLE
- RESOURCE AVAILABILITY
  - Lead contact
  - Materials availability
  - Data and code availability
- EXPERIMENTAL MODEL AND STUDY PARTICIPANT DETAILS
- METHOD DETAILS
  - Phylogenetic reconstruction
  - Egg morphology
  - Adult female morphology
  - Ecological data
  - Life history data
  - Egg metabolic rate measurements
  - Egg rates of water loss
- QUANTIFICATION AND STATISTICAL ANALYSIS
  - Phylogenetic analyses and hypothesis testing
  - Phylogenetic path analyses
  - Analysis of metabolic data
  - Analysis of rates of water loss data

SUPPLEMENTAL INFORMATION

Supplemental information can be found online at https://doi.org/10.1016/j.cub.2024.05.042.

ACKNOWLEDGMENTS

We thank François Tetaert for allowing us to use his image database of stick insect eggs (http://phasmatodea.fr/), Garret Jolma for help in the lab developing early water-loss protocols, Brenna Shea and The Missoula Insectarium for providing fresh eggs of several phasmid species, Brandon S. Cooper for use of the MAVEn system, and Camille Thomas-Bulle and Douglas J. Emlen for insightful discussions on the manuscript. We also thank three reviewers for their comments on the manuscript. This project received no specific funding.

AUTHOR CONTRIBUTIONS

Conceptualization, R.P.B. and H.A.W.; methodology, R.P.B. and H.A.W.; investigation, R.P.B.; formal analysis, R.P.B. and H.A.W.; visualization, R.P.B.; writing – original draft, R.P.B. and H.A.W.; writing – review & editing, R.P.B. and H.A.W.

DECLARATION OF INTERESTS

The authors declare no competing interests.

Received: November 19, 2023
Revised: March 14, 2024
Accepted: May 22, 2024
Published: June 18, 2024

REFERENCES

1. Hinton, H.E. (1981). Biology of Insect Eggs (Pergamon Press).
2. Donoughe, S. (2022). Insect egg morphology: evolution, development, and ecology. Curr. Opin. Insect Sci. *50*, 100868. https://doi.org/10.1016/j.cois.2021.12.008.
3. Stoddard, M.C., Yong, E.H., Akkaynak, D., Sheard, C., Tobias, J.A., and Mahadevan, L. (2017). Avian egg shape: form, function, and evolution. Science *356*, 1249–1254. https://doi.org/10.1126/science.aaj1945.
4. Kratochvil, L., and Frynta, D. (2006). Egg shape and size allometry in geckos (Squamata: Gekkota), lizards with contrasting eggshell structure: why lay spherical eggs? J. Zool. Syst. Evol. Res. *44*, 217–222. https://doi.org/10.1111/j.1439-0469.2005.00339.x.
5. Sargent, R.C., Taylor, P.D., and Gross, M.R. (1987). Parental care and the evolution of egg size in fishes. Am. Nat. *129*, 32–46. https://doi.org/10.1086/284621.
6. Marshall, D.J., and Keough, M.J. (2007). The evolutionary ecology of offspring size in marine invertebrates. Adv. Mar. Biol. *53*, 1–60. https://doi.org/10.1016/S0065-2881(07)53001-4.
7. Moran, A.L., and McAlister, J.S. (2009). Egg size as a life history character of marine invertebrates: is it all it's cracked up to be? Biol. Bull. *216*, 226–242. https://doi.org/10.1086/BBLv216n3p226.
8. Church, S.H., Donoughe, S., de Medeiros, B.A.S., and Extavour, C.G. (2019). Insect egg size and shape evolve with ecology but not developmental rate. Nature *571*, 58–62. https://doi.org/10.1038/s41586-019-1302-4.
9. García-Barros, E., and Munguira, M.L. (1997). Uncertain branch lengths, taxonomic sampling error, and the egg to body size allometry in temperate butterflies (Lepidoptera). Biol. J. Linn. Soc. *61*, 201–221. https://doi.org/10.1111/j.1095-8312.1997.tb01787.x.

10. Blackburn, T.M. (1991). An interspecific relationship between egg size and clutch size in bird. Auk *108*, 973–977.

11. Steele, D.H., and Steele, V.J. (1975). Egg size and duration of embryonic development in Crustacea. Int. Rev. Gesamten Hydrobiol. Hydrogr. *60*, 711–715. https://doi.org/10.1002/iroh.19750600609.

12. Gillooly, J.F., and Dodson, S.I. (2000). The relationship of egg size and incubation temperature to embryonic development time in univoltine and multivoltine aquatic insects. Freshw. Biol. *44*, 595–604. https://doi.org/10.1046/J.1365-2427.2000.00607.X.

13. Maino, J.L., Pirtle, E.I., and Kearney, M.R. (2017). The effect of egg size on hatch time and metabolic rate: theoretical and empirical insights on developing insect embryos. Funct. Ecol. *31*, 227–234. https://doi.org/10.1111/1365-2435.12702.

14. Balon, E.K. (1984). Patterns in the evolution of reproductive styles in fishes. In Fish Reproduction: Strategies and Tactics, G.W. Potts, and R.J. Wooton, eds. (Academic Press), pp. 35–53.

15. Paine, M.D. (1984). Ecological and evolutionary aspects of the early ontogeny of darters (Percidae: Etheostamatini). Environ. Biol. Fishes *11*, 97–106. https://doi.org/10.1007/BF00002258.

16. Rahn, H., and Ar, A. (1974). The avian egg: incubation time and water loss. Condor *76*, 147–152. https://doi.org/10.2307/1366724.

17. White, C.R., and Seymour, R.S. (2005). Allometric scaling of mammalian metabolism. J. Exp. Biol. *208*, 1611–1619. https://doi.org/10.1242/jeb.01501.

18. Glazier, D.S. (2010). A unifying explanation for diverse metabolic scaling in animals and plants. Biol. Rev. Camb. Philos. Soc. *85*, 111–138. https://doi.org/10.1111/j.1469-185X.2009.00095.x.

19. Maino, J.L., and Kearney, M.R. (2014). Ontogenetic and interspecific metabolic scaling in insects. Am. Nat. *184*, 695–701. https://doi.org/10.1086/678401.

20. Czesak, M.E., and Fox, C.W. (2003). Evolutionary ecology of egg size and number in a seed beetle: genetic trade-off differs between environments. Evolution *57*, 1121–1132. https://doi.org/10.1111/j.0014-3820.2003.tb00321.x.

21. Gibbs, M., Lace, L.A., Jones, M.J., and Moore, A.J. (2005). Egg size-number trade-off and a decline in oviposition site choice quality: female *Pararge aegeria* butterflies pay a cost of having males present at oviposition. J. Insect Sci. *5*, 39. https://doi.org/10.1093/jis/5.1.39.

22. Koch, L.K., and Meunier, J. (2014). Mother and offspring fitness in an insect with maternal care: phenotypic trade-offs between egg number, egg mass and egg care. BMC Evol. Biol. *14*, 125. https://doi.org/10.1186/1471-2148-14-125.

23. Berrigan, D. (1991). The allometry of egg size and number in insects. Oikos *60*, 313–321. https://doi.org/10.2307/3545073.

24. García-Barros, E. (2000). Body size, egg size, and their interspecific relationships with ecological and life history traits in butterflies (Lepidoptera: Papilionoidea, Hesperioidea). Biol. J. Linn. Soc. *70*, 251–284. https://doi.org/10.1111/j.1095-8312.2000.tb00210.x.

25. Woods, H.A., and Hill, R.I. (2004). Temperature-dependent oxygen limitation in insect eggs. J. Exp. Biol. *207*, 2267–2276. https://doi.org/10.1242/jeb.00991.

26. Woods, H.A. (2010). Water loss and gas exchange by eggs of *Manduca sexta*: trading off costs and benefits. J. Insect Physiol. *56*, 480–487. https://doi.org/10.1016/j.jinsphys.2009.05.020.

27. Eisner, T., Eisner, M., Rossini, C., Iyengar, V.K., Roach, B.L., Benedikt, E., and Meinwald, J. (2000). Chemical defense against predation in an insect egg. Proc. Natl. Acad. Sci. USA *97*, 1634–1639. https://doi.org/10.1073/pnas.030532797.

28. Guerra-Grenier, E. (2019). Evolutionary ecology of insect egg coloration: a review. Evol. Ecol. *33*, 1–19. https://doi.org/10.1007/s10682-018-09967-8.

29. Stoddard, M.C., Sheard, C., Akkaynak, D., Yong, E.H., Mahadevan, L., and Tobias, J.A. (2019). Evolution of avian egg shape: underlying mechanisms and the importance of taxonomic scale. Ibis *161*, 922–925. https://doi.org/10.1111/IBI.12755.

30. Simon, S., Letsch, H., Bank, S., Buckley, T.R., Donath, A., Liu, S., Machida, R., Meusemann, K., Misof, B., Podsiadlowski, L., et al. (2019). Old world and new world Phasmatodea: phylogenomics resolve the evolutionary history of stick and leaf insects. Front. Ecol. Evol. *7*, 1–14. https://doi.org/10.3389/fevo.2019.00345.

31. Robertson, J.A., Bradler, S., and Whiting, M.F. (2018). Evolution of oviposition techniques in stick and leaf insects (Phasmatodea). Front. Ecol. Evol. *6*, 1–15. https://doi.org/10.3389/fevo.2018.00216.

32. Tihelka, E., Cai, C., Giacomelli, M., Pisani, D., and Donoghue, P.C.J. (2020). Integrated phylogenomic and fossil evidence of stick and leaf insects (Phasmatodea) reveal a Permian–Triassic co-origination with insectivores. R. Soc. Open Sci. *7*, 201689. https://doi.org/10.1098/rsos.201689.

33. Brock, P.D., Büscher, T.H., and Baker, E. (2021). Phasmida Species File Online. Version 5050. Phasmida Species File. http://phasmida.speciesfile.org.

34. Boisseau, R.P., Bradler, S., and Emlen, D.J. (2023). Divergence time and environmental similarity predict the strength of morphological convergence in stick and leaf insects. Preprint at bioRxiv. https://doi.org/10.1101/2023.11.07.565940.

35. Büscher, T.H., Reck, L.M., and Gorb, S.N. (2024). Functional surface structures on the eggs of stick and leaf insects (Insecta: Phasmatodea). Zoologica *166*, 1–278.

36. Hennemann, F.H., Conle, O.V., Brock, P.D., and Seow-Choen, F. (2016). Revision of the Oriental subfamily Heteropteryginae kirby, 1896, with a re-arrangement of the family Heteropterygidae and the descriptions of five new species of *Haaniella* kirby, 1904. (Phasmatodea: Areolatae: Heteropterygidae). Zootaxa *4159*, 1–219. https://doi.org/10.11646/zootaxa.4159.1.1.

37. Seiler, C., Bradler, S., and Koch, R. (2000). Ratgeber Phasmiden: Pflege und Zucht von Gespenstschrecken, Stabschrecken und Wandelnden Blättern im Terrarium (Bede-Verlag).

38. O'Hanlon, J.C., Jones, B.R., and Bulbert, M.W. (2020). The dynamic eggs of the Phasmatodea and their apparent convergence with plants. Sci. Nat. *107*, 1–12. https://doi.org/10.1007/s00114-020-01690-1.

39. Kobayashi, S., Usui, R., Nomoto, K., Ushirokita, M., Denda, T., and Izawa, M. (2014). Does egg dispersal occur via the ocean in the stick insect *Megacrania tsudai* (Phasmida: Phasmatidae)? Ecol. Res. *29*, 1025–1032. https://doi.org/10.1007/S11284-014-1188-4.

40. Stanton, A.O., Dias, D.A., and O'Hanlon, J.C. (2015). Egg dispersal in the Phasmatodea: convergence in chemical signaling strategies between plants and animals? J. Chem. Ecol. *41*, 689–695. https://doi.org/10.1007/s10886-015-0604-8.

41. Smart, H.R., Andrew, N.R., and O'Hanlon, J.C. (2023). Ant mediated dispersal of spiny stick insect (Extatosoma tiaratum) eggs and Acacia longifolia seeds is ant-species dependent. Aust. J. Zool. *70*, 105–114. https://doi.org/10.1071/ZO22036.

42. Suetsugu, K., Funaki, S., Takahashi, A., Ito, K., and Yokoyama, T. (2018). Potential role of bird predation in the dispersal of otherwise flightless stick insects. Ecology *99*, 1504–1506. https://doi.org/10.1002/ECY.2230.

43. Suetsugu, K., Nozaki, T., Hirota, S.K., Funaki, S., Ito, K., Isagi, Y., Suyama, Y., and Kaneko, S. (2023). Phylogeographical evidence for historical long-distance dispersal in the flightless stick insect *Ramulus mikado*. Proc. Biol. Sci. *290*, 20231708. https://doi.org/10.1098/rspb.2023.1708.

44. Goldberg, J., Bresseel, J., Constant, J., Kneubühler, B., Leubner, F., Michalik, P., and Bradler, S. (2015). Extreme convergence in egg-laying strategy across insect orders. Sci. Rep. *5*, 7825. https://doi.org/10.1038/srep07825.

45. Severin, H.H.P. (1910). A study on the structure of the egg of the walking-stick, *Diapheromera femorata* Say; and the biological significance of the

resemblance of phasmid eggs to seeds. Ann. Entomol. Soc. Am. *3*, 83–92. https://doi.org/10.1093/aesa/3.2.83.

46. Henneguy, L.F. (1890). Note sur la structure de l'enveloppe de l'oeuf des Phyllies. Bull. Société Philomanthique Paris *2*, 18–25.
47. Sharp, D. (1898). Account of the Phasmidae, with notes on the eggs. In Zoological Results Based on Material Collected in New Britain, New Guinea, Loyalty Islands and Elsewhere, A. Willey, ed. (Cambridge University Press).
48. Brock, P.D., and Hasenpusch, J.W. (2009). The Complete Field Guide to Stick and Leaf Insects of Australia (CSIRO Publishing).
49. Brock, P.D. (2000). A Complete Guide to Breeding Stick and Leaf Insects (TFH Publications).
50. Woods, H.A., Bonnecaze, R.T., and Zrubek, B. (2005). Oxygen and water flux across eggshells of *Manduca sexta*. J. Exp. Biol. *208*, 1297–1308. https://doi.org/10.1242/JEB.01525.
51. Biewener, A.A., and Patek, S.N. (2018). Animal Locomotion (Oxford University Press).
52. Boisseau, R.P., Büscher, T.H., Klawitter, L.J., Gorb, S.N., Emlen, D.J., and Tobalske, B.W. (2022). Multi-modal locomotor costs favor smaller males in a sexually dimorphic leaf-mimicking insect. BMC Ecol. Evol. *22*, 39. https://doi.org/10.1186/s12862-022-01993-z.
53. Whiting, M.F., Bradler, S., and Maxwell, T. (2003). Loss and recovery of wings in stick insects. Nature *421*, 264–267. https://doi.org/10.1038/nature01313.
54. Bank, S., and Bradler, S. (2022). A second view on the evolution of flight in stick and leaf insects (Phasmatodea). BMC Ecol. Evol. *22*, 62. https://doi.org/10.1186/S12862-022-02018-5.
55. Forni, G., Martelossi, J., Valero, P., Hennemann, F.H., Conle, O., Luchetti, A., and Mantovani, B. (2022). Macroevolutionary analyses provide new evidence of phasmid wings evolution as a reversible process. Syst. Biol. *71*, 1471–1486. https://doi.org/10.1093/SYSBIO/SYAC038.
56. Rahn, H., Paganelli, C.V., and Ar, A. (1974). The avian egg: air-cell gas tension, metabolism and incubation time. Respir. Physiol. *22*, 297–309. https://doi.org/10.1016/0034-5687(74)90079-6.
57. Vleck, C.M., and Hoyt, D.F. (1991). Metabolism and energetics of reptilian and avian embryos. In Egg Incubation: Its Effects on Embryonic Development in Birds and Reptiles, D.C. Deeming, and M.W.J. Ferguson, eds. (Cambridge University Press), pp. 285–306.
58. Hoyt, D.F., and Rahn, H. (1980). Respiration of avian embryos - A comparative analysis. Respir. Physiol. *39*, 255–264. https://doi.org/10.1016/0034-5687(80)90057-2.
59. Mortola, J.P. (2009). Gas exchange in avian embryos and hatchlings. Comp. Biochem. Physiol. A Mol. Integr. Physiol. *153*, 359–377. https://doi.org/10.1016/J.CBPA.2009.02.041.
60. Pettersen, A.K., Schuster, L., and Metcalfe, N.B. (2022). The evolution of offspring size: a metabolic scaling perspective. Integr. Comp. Biol. *62*, 1492–1502. https://doi.org/10.1093/ICB/ICAC076.
61. Numata, H., and Shintani, Y. (2023). Diapause in univoltine and semivoltine life cycles. Annu. Rev. Entomol. *68*, 257–276. https://doi.org/10.1146/annurev-ento-120220-101047.
62. Ar, A., and Rahn, H. (1980). Water in the avian egg: overall budget of incubation. Am. Zool. *20*, 373–384. https://doi.org/10.1093/ICB/20.2.373.
63. García-Barros, E. (2006). Within and between species scaling in the weight, water, carbon and nitrogen contents of eggs and neonate larvae of twelve satyrine butterflies (Lepidoptera: Nymphalidae). Eur. J. Entomol. *103*, 559–568. https://doi.org/10.14411/EJE.2006.076.
64. Coleman, D.C., and Crossley, D.A., Jr. (2004). Fundamentals of Soil Ecology (Academic Press).
65. Sprague, J.C., and Woods, H.A. (2015). Costs and benefits of underground pupal chambers constructed by insects: a test using *Manduca sexta*. Physiol. Biochem. Zool. *88*, 521–534. https://doi.org/10.1086/682251.
66. Hall, S.J., and Silver, W.L. (2013). Iron oxidation stimulates organic matter decomposition in humid tropical forest soils. Glob. Change Biol. *19*, 2804–2813. https://doi.org/10.1111/GCB.12229.
67. Kolm, N., and Ahnesjö, I. (2005). Do egg size and parental care coevolve in fishes? J. Fish Biol. *66*, 1499–1515. https://doi.org/10.1111/J.0022-1112.2005.00777.X.
68. Summers, K., McKeon, C.S., and Heying, H. (2005). The evolution of parental care and egg size: a comparative analysis in frogs. Proc. R. Soc. Lond. B *273*, 687–692. https://doi.org/10.1098/RSPB.2005.3368.
69. Nussbaum, R.A., and Schultz, D.L. (1989). Coevolution of parental care and egg size. Am. Nat. *133*, 591–603. https://doi.org/10.1086/284939.
70. Gilbert, J.D.J., and Manica, A. (2010). Parental care trade-offs and life-history relationships in insects. Am. Nat. *176*, 212–226. https://doi.org/10.1086/653661.
71. Schwabl, H., Palacios, M.G., and Martin, T.E. (2007). Selection for rapid embryo development correlates with embryo exposure to maternal androgens among passerine birds. Am. Nat. *170*, 196–206. https://doi.org/10.1086/519397.
72. Silver, W.L., Lugo, A.E., and Keller, M. (1999). Soil oxygen availability and biogeochemistry along rainfall and topographic gradients in upland wet tropical forest soils. Biogeochemistry *44*, 301–328. https://doi.org/10.1007/BF00996995.
73. Büscher, T.H., Quigley, E., and Gorb, S.N. (2020). Adhesion performance in the eggs of the Philippine leaf insect *Phyllium philippinicum* (Phasmatodea: Phylliidae). Insects *11*, 400. https://doi.org/10.3390/insects11070400.
74. Büscher, T.H., Bank, S., Cumming, R.T., Gorb, S.N., and Bradler, S. (2023). Leaves that walk and eggs that stick: comparative functional morphology and evolution of the adhesive system of leaf insect eggs (Phasmatodea: Phylliidae). BMC Ecol. Evol. *23*, 17. https://doi.org/10.1186/S12862-023-02119-9.
75. Montgomerie, R., Hemmings, N., Thompson, J.E., and Birkhead, T.R. (2021). The shapes of birds' eggs: evolutionary constraints and adaptations. Am. Nat. *198*, E215–E231. https://doi.org/10.1086/716928.
76. Günther, K. (1953). Über die taxonomische Gliederung und die geographische Verbreitung der Insektenordnung der Phasmatodea. Contrib. Entomol. *3*, 541–563. https://doi.org/10.21248/contrib.entomol.3.5.541-563.
77. Bedford, G.O. (1978). Biology and ecology of the Phasmatodea. Annu. Rev. Entomol. *23*, 125–149. https://doi.org/10.1146/annurev.en.23.010178.001013.
78. Brock, P.D., and Büscher, T.H. (2022). Stick and Leaf-Insects of the World (NAP Editions).
79. Fischer, K., Brakefield, P.M., and Zwaan, B.J. (2003). Plasticity in butterfly egg size: why larger offspring at lower temperatures? Ecology *84*, 3138–3147. https://doi.org/10.1890/02-0733.
80. Kojima, W., and Lin, C.P. (2022). Non-linear latitudinal cline of egg size and its consequence for larval survival in the rhinoceros beetle. Biol. J. Linn. Soc. *136*, 375–383. https://doi.org/10.1093/biolinnean/blac020.
81. Potter, K.A., Arthur Woods, H.A., and Pincebourde, S. (2013). Microclimatic challenges in global change biology. Glob. Change Biol. *19*, 2932–2939. https://doi.org/10.1111/gcb.12257.
82. Pincebourde, S., and Woods, H.A. (2012). Climate uncertainty on leaf surfaces: the biophysics of leaf microclimates and their consequences for leaf-dwelling organisms. Funct. Ecol. *26*, 844–853. https://doi.org/10.1111/j.1365-2435.2012.02013.x.
83. Boisseau, R.P., and Woods, H.A. (2024). Resource allocation strategies and mechanical constraints drive the diversification of stick and leaf insect eggs. Preprint at bioRxiv. https://doi.org/10.1101/2023.11.10.566544.
84. R Core Team (2021). R: A Language and Environment for Statistical Computing (R Foundation for Statistical Computing).

85. Hijmans, R.J. (2021). raster: Geographic Data Analysis and Modeling. R package version 3.6-26. https://cran.r-project.org/web/packages/raster/raster.pdf.

86. Revell, L.J. (2012). phytools: an R package for phylogenetic comparative biology (and other things). Methods Ecol. Evol. *3*, 217–223. https://doi.org/10.1111/j.2041-210X.2011.00169.x.

87. Pinheiro, J., Bates, D., DebRoy, S., and Sarkar, D.; R Core Team (2021). Nlme: linear and nonlinear mixed effects models. R package version 3.1-162.

88. Paradis, E., and Schliep, K. (2019). ape 5.0: an environment for modern phylogenetics and evolutionary analyses in R. Bioinformatics *35*, 526–528. https://doi.org/10.1093/bioinformatics/bty633.

89. Lenth, R. (2019). Emmeans: estimated Marginal Means, aka Least-Squares Means. R package version 1.4.

90. van der Bijl, W. (2018). phylopath: easy phylogenetic path analysis in R. PeerJ *6*, e4718. https://doi.org/10.7717/peerj.4718.

91. Wood, S.N. (2017). Generalized Additive Models: an Introduction with R (CRC Press).

92. Bates, D., Mächler, M., Bolker, B., and Walker, S. (2015). Fitting linear mixed-effects models using lme4. J. Stat. Softw. *67*, 1–48. https://doi.org/10.18637/jss.v067.i01.

93. Bradler, S., and Buckley, T.R. (2018). Biodiversity of Phasmatodea. In Insect Biodiversity: Science and Society, R.G. Foottit, and P.H. Adler, eds. (Wiley-Blackwell), pp. 281–313.

94. Bouckaert, R., Heled, J., Kühnert, D., Vaughan, T., Wu, C.H., Xie, D., Suchard, M.A., Rambaut, A., and Drummond, A.J. (2014). BEAST 2: A software platform for Bayesian evolutionary analysis. PLoS Comput. Biol. *10*, e1003537. https://doi.org/10.1371/journal.pcbi.1003537.

95. Church, S.H., Donoughe, S., de Medeiros, B.A.S., and Extavour, C.G. (2019). A dataset of egg size and shape from more than 6,700 insect species. Sci. Data *6*, 104. https://doi.org/10.1038/s41597-019-0049-y.

96. Arai, M., and Yago, M. (2015). Curious oviposition behavior in *Phyllium westwoodii* (Phasmatodea: Phylliidae): preliminary observations. J. Insect Sci. *15*, 135. https://doi.org/10.1093/jisesa/iev111.

97. Fick, S.E., and Hijmans, R.J. (2017). WorldClim 2: new 1-km spatial resolution climate surfaces for global land areas. Int. J. Climatol. *37*, 4302–4315. https://doi.org/10.1002/joc.5086.

98. van Velthuizen, H., Huddleston, B., Fischer, G., Salvatore, M., Ataman, E., Nachtergaele, F.O., Zanetti, M., Bloise, M., Gis, F., Antonicelli, A., et al. (2007). Mapping Biophysical Factors That Influence Agricultural Production and Rural Vulnerability (Food and Agriculture Organization of the United Nations and International Institute for Applied Systems Analysis).

99. Kuntz, S.G., and Eisen, M.B. (2014). *Drosophila* embryogenesis scales uniformly across temperature in developmentally diverse species. PLoS Genet. *10*, e1004293. https://doi.org/10.1371/journal.pgen.1004293.

100. Kobayashi, S., Usui, R., Nomoto, K., Ushirokita, M., Denda, T., and Izawa, M. (2016). Population dynamics and the effects of temperature on the eggs of the seawater-dispersed stick insect *Megacrania tsudai* (Phasmida: Phasmatidae). Zool. Stud. *55*, e20. https://doi.org/10.6620/ZS.2016.55-20.

101. Kim, M.J., Kim, K.E., Son, S., Park, Y., Nam, Y., and Jung, J.K. (2023). Development of a phenology model for egg hatching of walking-stick insect, *Ramulus mikado* (Phasmatodea: Phasmatidae) in Korea. Forests *14*, 1710. https://doi.org/10.3390/f14091710.

102. Gillooly, J.F., Brown, J.H., West, G.B., Savage, V.M., and Charnov, E.L. (2001). Effects of size and temperature on metabolic rate. Science *293*, 2248–2251. https://doi.org/10.1126/science.1061967.

103. Winston, P.W., and Bates, D.H. (1960). Saturated solutions for the control of humidity in biological research. Ecology *41*, 232–237. https://doi.org/10.2307/1931961.

104. Zeng, Y., O'Malley, C.O., Singhal, S., Rahim, F., Park, S., Chen, X., and Dudley, R. (2020). A tale of winglets: evolution of flight morphology in stick insects. Front. Ecol. Evol. *8*, 1–15. https://doi.org/10.3389/fevo.2020.00121.

105. von Hardenberg, A., and Gonzalez-Voyer, A. (2013). Disentangling evolutionary cause-effect relationships with phylogenetic confirmatory path analysis. Evolution *67*, 378–387. https://doi.org/10.1111/j.1558-5646.2012.01790.x.

106. Gonzalez-Voyer, A., and von Hardenberg, A. (2014). An introduction to phylogenetic path analysis. In Modern Phylogenetic Comparative Methods and Their Application in Evolutionary Biology: Concepts and Practice, L.Z. Garamszegi, ed. (Springer-Verlag), pp. 201–229. https://doi.org/10.1007/978-3-662-43550-2_8.

107. Lleras, C. (2005). Path analysis. In Encyclopedia of Social Measurement, K. Kempf-Leonard, ed. (Elsevier), pp. 25–30. https://doi.org/10.1016/B0-12-369398-5/00483-7.

108. Crespi, B.J. (2004). Vicious circles: positive feedback in major evolutionary and ecological transitions. Trends Ecol. Evol. *19*, 627–633. https://doi.org/10.1016/j.tree.2004.10.001.

STAR★METHODS

KEY RESOURCES TABLE

REAGENT or RESOURCE	SOURCE	IDENTIFIER
Biological samples		
List of all specimens from other studies and associated Genbank accession numbers used to build phylogenetic tree	This paper	Dataset S1[83]; https://zenodo.org/records/11146647
List of egg specimen images used to measure morphological traits for all species and associated ecological traits	This paper	Dataset S1[83]; https://zenodo.org/records/11146647
Eggs of *Eurycantha calcarata* (Kimbe, West New Britain, Papua New Guinea)(*n*=16)	Culture stock (Missoula Butterfly house & Insectarium, Missoula MT, USA)	calcarata #1-16
Eggs of *Extatosoma tiaratum* (Queensland, Australia) (*n*=16)	Culture stock (Missoula Butterfly house & Insectarium, Missoula MT, USA)	tiaratum #1-16
Eggs of *Heteropteryx dilatata* (Cameron Highlands, Malaysia) (*n*=16)	Culture stock (Missoula Butterfly house & Insectarium, Missoula MT, USA)	dilatata #1-16
Eggs of *Medauroidea extradentata* (Vietnam) (n=16)	Culture stock (Missoula Butterfly house & Insectarium, Missoula MT, USA)	extradentata #1-16
Eggs of *Phyllium philippinicum* (Zambales, Philippines) (n=16)	Culture stock (Audubon Insectarium, New Orleans, LA, USA)	philippinicum #1-16
Chemicals, peptides, and recombinant proteins		
CO2-free air	NorLab, Norco, Boise, ID, USA	Zero Air NLB 2550
25 ppm CO_2 in N_2	NorLab, Norco, Boise, ID, USA	Custom-made tank
Deposited data		
Phylogenetic tree	Boisseau et al.[34]	Phasmid_MCCphylogeny[83]; https://zenodo.org/records/11146647
All comparative data	This paper	Dataset S1[83]; https://zenodo.org/records/11146647
All R scripts	This paper	Boisseau and Woods[83]; https://zenodo.org/records/11146647
All metabolic rate and water loss data	This paper	Dataset S1[83]; https://zenodo.org/records/11146647
Raw respirometry data	This paper	Boisseau and Woods[83]; https://zenodo.org/records/11146647
Software and algorithms		
R software v4.1.1	R core Team[84]	https://www.r-project.org/
R package: raster v3.6-26	Hijmans[85]	https://cran.r-project.org/web/packages/raster/index.html
R package: phytools v1.5-1	Revell[86]	https://cran.r-project.org/web/packages/phytools/index.html
R package: nlme v3.1-162	Pinheiro et al.[87]	https://cran.r-project.org/web/packages/nlme/index.html
R package: ape v5.7-1	Paradis and Schliep[88]	https://cran.r-project.org/web/packages/ape/index.html
R package: emmeans v1.8.7	Lenth[89]	https://cran.r-project.org/web/packages/emmeans/index.html
R package: phylopath v1.1.3	van der Bijl[90]	https://cran.r-project.org/web/packages/phylopath/index.html
R package: mgcv v1.8-42	Wood[91]	https://cran.r-project.org/web/packages/mgcv/index.html

(*Continued on next page*)

Continued

REAGENT or RESOURCE	SOURCE	IDENTIFIER
R package: lme4 v1.1-33	Bates et al.[92]	https://cran.r-project.org/web/packages/lme4/index.html
Other		
Multiple animal versatile energetics flow through system	Sable Systems International, North Las Vegas, NV, USA	MAVEn-FT
CO_2/H_2O analyzer	Licor, Lincoln, NE, USA	LI-7000
Analytical balance	Mettler Toledo, Columbus, OH, USA	ME104TE/00
Microbalance	Sartorius AG, Göttingen, Germany	MC5

RESOURCE AVAILABILITY

Lead contact

Further information and requests for resources should be directed to and will be fulfilled by the lead contact, Romain Boisseau (romain.boisseau@unil.ch)

Materials availability

This study did not generate new unique reagents.

Data and code availability

- The data that support the findings of this study have been deposited at Zenodo and are publicly available as of the date of publication, under the DOI: https://doi.org/10.5281/zenodo.11146647.
- All original code has also been deposited at Zenodo and is publicly available as of the date of publication under the same DOI as for the datasets: https://doi.org/10.5281/zenodo.11146647.
- Any additional information required to reanalyze the data reported in this paper is available from the lead contact upon request.

EXPERIMENTAL MODEL AND STUDY PARTICIPANT DETAILS

Stick and leaf insects are a group of approximately 3500 described species of large, mostly nocturnal terrestrial herbivores mainly distributed in tropical and subtropical regions.[33] They are renowned for their impressive forms of visual camouflage, many species mimicking various parts of plants, such as twigs, bark and leaves. Phasmid eggs differ from other insect eggs because they possess a strong, hardened outer shell, analogous to the shell of bird eggs, that likely enabled the formation of diverse shapes and structures.[78] Phasmid species are generally easy to keep in captivity as they are often able to thrive on a wide variety of alternative food plants.[93] Thus, these charismatic insects are often exhibited in zoos, museums, or school classes. Most of the knowledge on phasmatodean traits comes from such breeding cultures and observations made by enthusiastic amateur entomologists.[37,49]

For our comparative analyses, we relied on high quality photographs of eggs from the literature and online databases and trait data collected from the scientific literature and amateur records. For our physiological metabolic rate and water loss measurements, we worked on freshly laid eggs from five unrelated species belonging to separate subfamilies (main clades): *Eurycantha calcarata* (Lucas, 1869; subfamily Lonchodinae), *Extatosoma tiaratum* (Macleay, 1826; subfamily Phasmatinae: "Lanceocercata"), *Heteropteryx dilatata* (Parkinson, 1798; subfamily Heteropteryginae), *Medauroidea extradentata* (Brunner von Wattenwyl, 1907; subfamily Clitumninae) and *Phyllium philippinicum* (Hennemann, Conle, Gottardo & Bresseel, 2009; subfamily Phyllinae). These specimens were obtained from culture stocks of the Missoula Butterfly House & Insectarium (Missoula, MT, USA) and of the Audubon Insectarium (New Orleans, LA, USA) that were initially collected in: Kimbe, West New Britain, Papua New Guinea in 1977 (*E. calcarata*); Queensland, Australia in the 1970s (*E. tiaratum*); Tanah Rata, Cameron Highlands, Malaysia in 1974 (*H. dilatata*); Vietnam in the 1950s (*M. extradentata*) and Subic, Zambales, Eastern Luzon, Philippines in 2001 (*P. philippinicum*). *E. calcarata* were fed fresh maple leaves (*Acer platanoides*); *E. tiaratum*, *H. dilatata*, *P. philippinicum* fresh bramble and raspberry leaves (*Rubus armeniacus*, *Rubus idaeus*); and *M. extradentata* fresh organic lettuce leaves. Nymphs and adults of all species were kept at room temperature (21 - 23°C) in large mesh cages (40cm x 40cm x 70cm high) containing no more than 50 individuals, sprayed lightly with water once a day, and under a 12h/12h light-dark cycle. All eggs were fertilized except *M. extradentata* eggs, which were obtained from a parthenogenetic culture. *P. philippinicum*, *M. extradentata* and *E. tiaratum* females typically drop or flick their eggs away during oviposition while *E. calcarata* and *H. dilatata* bury them.[31] The two later species were provided with a tray containing moist sand for females to lay their eggs in. 16 eggs were sampled less than 24h after being laid for each species. Throughout embryonic development, eggs were kept individually in separate wells of a plastic 24-well plate placed inside a plastic box whose bottom was filled with water to maintain nearly 100% relative humidity around the eggs. The eggs were kept at room temperature (21 - 23°C) under a natural day/night cycle until hatching.

METHOD DETAILS

Phylogenetic reconstruction

For the present study, we used a phylogeny from a study dealing with morphological convergence in adult female stick insects,[34] which includes a total of 314 phasmid taxa (~9% of phasmid species diversity and ~33% of all described genera) and one embiopteran species as outgroup (i.e., from the sister clade of Phasmatodea). The phylogenetic analyses were originally performed using genetic data from 3 nuclear (*i.e.,* 18S rRNA, 28S rRNA and histone subunit 3) and 4 mitochondrial genes (*i.e.,* 12S rRNA, 16S rRNA, cytochrome-c oxidase subunit I and II) and Bayesian inferences (BEAST2, v. 2.6.3[94]). The basal backbone topology of the tree was constrained to match that of transcriptome-based studies that could confidently infer the deep relationships between all the major clades of Phasmatodea.[30,32] The resulting maximum clade credibility tree was overall strongly supported and congruent with previous phylogenetic reconstructions.[31,34,44,54]

Egg morphology

We collected high quality photographs or drawings of eggs in dorsal and lateral view for a total of 144 different species included in the phylogeny mainly from the egg picture database of F. Tetaert (Office pour les insectes et leur environnement OPIE, France, retrieved from phasmatodea.fr in August 2021) and from the published literature and other online databases (see Dataset S1[83] for details). We applied the guided landmark-based methodology of Church and Donoughe et al.[95] to quantify egg shape traits (Figure S1A). We used the R software (v4.1.1)[84] and the package "raster,"[85] to measure egg length (L) from the base of the operculum to the posterior end of the egg, and width and height along three different latitudinal lines at ¼, ½ and ¾ (respectively w_1, w_2, w_3 and h_1, h_2, h_3) of the egg longitudinal axis (Figure S1A). Egg width (w) and height (h) were considered as the maximum values of w_1, w_2, w_3 and h_1, h_2, h_3 respectively. Egg volume was then estimated using the equation for the volume of an ellipsoid ($\frac{\pi}{6}lwh$). We verified the relevance of using this estimate of volume as our measure of egg size by regressing egg volume on egg mass (after $\log_{10}$-transformation) for species where that information could be collected (n = 76 species, see Dataset S1[83] for details). We found a strong correlation between the two (β=0.87 ± 0.04, p<0.0001, R^2=0.84, Figure S4) and therefore chose to use egg volume as our measure of egg size as it was available for more taxa (n = 144 species). Egg surface area (SA) was calculated as the surface area of an ellipsoid using the approximate formula:

$$SA = 4\pi \sqrt[1.6]{\frac{L^{1.6}w^{1.6}+L^{1.6}h^{1.6}+w^{1.6}h^{1.6}}{3}}$$

To characterize egg shape variation while controlling for size, we performed a phylogenetic Principal Component Analysis (pPCA, *R function*: "R package"; *phyl.pca*: "phytools"[86]) including L, w_1, w_2, w_3, h_1, h_2 and h_3, but original values were substituted with residuals calculated from a phylogenetically-corrected generalized least-squares (PGLS) regression against egg volume (*gls*: "nlme" and "ape,"[87,88] lambda='ML').

Adult female morphology

To quantify adult female size, we used data on adult female volume originally collected in a previous study (n = 207 species),[34] which estimated female body volume as an ellipsoid using the average body length, width, and height of a species. Original measurements were obtained from digital images of live and dried specimens. From this study, we also used the species average width of the female's ninth tergite (i.e., width the ninth abdominal dorsal plate) as it roughly corresponds to the location of the oviduct, from which eggs emerge during oviposition[96] and whose diameter may mechanically constrain egg morphology.

Ecological data

Using primarily the dataset assembled by Robertson et al.,[31] we classified egg oviposition strategies into three categories: females drop or flick eggs to the ground from higher up in the local canopy, bury eggs into soil or other soft substrates, or glue eggs to substrate (including eggs encased in an ootheca) (n = 208 species). We then mapped oviposition strategies onto the phylogeny and ran an ancestral state reconstruction using stochastic character mapping (*make.simmap*: "phytools"). We calculated the transition matrix using MCMC and assumed different transition between all states (model "ARD"). We subsequently simulated and summarized 1,000 stochastic character maps to obtain posterior probabilities for each state at each node.

We gathered observational data on the flight capacities of adult females across species. Female flight capacity was classified as either flight-capable (including gliding) or flightless (including parachuting) (Dataset S1,[83] n = 208 species).

We also collected climate data for each species (n = 207) based on current geographic distribution and corresponding to climate conditions experienced at the most central location of the range where the species have been collected (using the collection location of type specimens) or observed (using observations on iNaturalist, available from https://www.inaturalist.org, accessed July 2021). The dataset included annual mean temperature, mean diurnal range (i.e., mean of monthly (maximum - minimum temperature)), temperature seasonality (i.e., standard deviation × 100), annual temperature range (i.e., maximum temperature of warmest month - minimum temperature of coldest month), annual precipitation, precipitation seasonality (i.e., coefficient of variation) from worldclim.[97] The dataset also comprised the length of the growing period (number of days during a year when temperatures are above 5°C and precipitation exceeds half the potential evapotranspiration, available from https://data.apps.fao.org/map/catalog [98]), net

primary production of biomass (grams of dry matter per m^2 per year; Climate Research Unit, Univ. of East Anglia, period 1976-2000, FAO Map Catalog, available from https://data.apps.fao.org/map/catalog), and total annual growing degree days (a measure of the annual amount of thermal energy available for plant and insect growth; Climate Research Unit, Univ. of East Anglia, available from https://sage.nelson.wisc.edu/data-and-models). We then ran a principal component analysis to summarize climatic variation across the geographic distribution of the phasmids (*prcomp*: "stats"). We kept the first two axes of the PCA (climate PC1 and PC2, respectively, explaining 56% and 17% of the total variation) to quantify climatic variation between species (Figure S3). Climate PC1 reflected tropical versus temperate patterns differing in annual precipitation, annual temperature, and magnitude of diurnal and annual variation in temperature and consequently in net primary productivity (i.e., food availability for herbivorous insects). PC1 is overall high in tropical regions and low in more temperate and seasonal regions with restricted growing periods. Climate PC2 mostly represented variation in precipitation seasonality with regions showing strong shifts between dry and wet/monsoon seasons displaying a high PC2.

Life history data

We collected data on the average number of eggs laid by a female during its lifetime (n = 100 species) and on average embryonic development duration (from oviposition to hatching, n = 136 species) from the published literature, amateur breeding guides and the phasmid breeder community (Dataset S1[83]). We only included data from sources that reported incubation temperature as embryogenesis duration is typically dependent on temperature.[99–101] Data from many systems, including insects, suggest that the temperature-dependence of developmental rates is mainly due to the temperature-dependence of reaction kinetics.[102] Therefore, following previous work,[8,13,102] we standardized all embryonic development durations (DT) to a constant temperature of 20°C (T_{ref} = 293.15K) using the mean reported incubation temperature (T) and the Boltzmann-Arrhenius equation with E_i/k_B set to 8000K, where E_i is the activation energy and k_B is Boltzmann's constant:

$$Corrected\ DT = \frac{DT}{e^{\frac{E_i}{k_B}\left(\frac{1}{T_{ref}} - \frac{1}{T}\right)}}$$

Lifetime fecundity (i.e., egg number) was often estimated from reports of weekly egg numbers per female, multiplied by female adult longevity. Lifetime reproductive output was calculated as the product of egg volume and the fecundity (n = 96 species with sufficient data) and was used to quantify average female lifetime reproductive investment.

Egg metabolic rate measurements

Sixteen freshly laid eggs were obtained from five unrelated phasmid species from culture stocks: *Eurycantha calcarata*, *Extatosoma tiaratum*, *Heteropteryx dilatata*, *Medauroidea extradentata* and *Phyllium philippinicum*. Egg metabolic rate was estimated as the rate of CO_2 production using flow-through respirometry. CO_2 concentrations were measured using a Licor LI-7000 CO_2/H_2O analyzer (Licor, Lincoln, NE, USA) in differential mode associated with a 16-chamber flow-through respirometry and data acquisition system (MAVEn-FT, Sable Systems International, North Las Vegas, NV, USA). The analyzer was calibrated frequently using CO_2-free air and 25 ppm CO_2 in N_2 (NorLab, Norco, Boise, ID, USA). Air flow rates were set to 25 $ml.min^{-1}$ (standard temperature and pressure) in the 16 experimental chambers. Gases circulated between the instruments in 3 mm inner-diameter plastic tubing (Bevaline-IV, Cole Parmer, Vernon Hills, IL, USA). Dry, CO_2-free air was first directed through a column containing Drierite and Ascarite to trap residual CO_2, then through the reference cell of the analyzer (referred to as cell A), which measured the fractional CO_2 concentration in incurrent air. From there, the air current was hydrated passing it through a bottle containing water (and several beads of Ascarite to keep CO_2 levels low). The hydrated stream was then directed through egg-containing chambers in the MAVEn and back into the measurement side of the analyzer (referred to as cell B), which measured the fractional CO_2 concentration in excurrent air. Data from the system was logged at 1 Hz using the MAVEn software.

Approximately every two weeks, each of the 16 eggs per species was weighed on an analytical balance (ME104TE/00, Mettler Toledo, Columbus, OH, USA) and subsequently placed individually in the 16 experimental chambers between the hours of 1600 and 2000 and left to run overnight until 0800-1000. Within each MAVEn cycle, air flow was first directed to the baseline channel for 5 min then to two experimental chambers sequentially for 20 min each and back to the baseline channel and so on through the remaining chambers.

Egg rates of water loss

To assess rates of water loss, we held freshly laid eggs of the five species in a Tupperware container at 75% relative humidity (at room temperature 21 – 23°C). Humidity was controlled by filling the bottom of each container with saturated solutions of sodium chloride in water,[103] and eggs were held in 24-well plates positioned above the salt solutions. For controls, we used the eggs held in 100% relative humidity on which we measured metabolic rates. Depending on their size, eggs were weighed twice per week on either a Mettler Toledo ME54TE/00 (± 0.1 mg) or a Sartorius MC-5 microbalance (± 1 μg). For the first species examined (*E. calcarata*), we measured water loss over the entirety of the developmental period (∼ 126 days). For each egg, we calculated water loss rate as the slope of the linear regression between egg mass and time. This species showed no changes in rate of water loss over time (Figure S2C), so for the four other species we measured water loss for just the first 35 days of development. At the end of the measurement period, eggs were

transferred to a drying oven (60°C) for two weeks and then reweighed dry. From these data and the initial fresh masses, we calculated initial water contents.

QUANTIFICATION AND STATISTICAL ANALYSIS

Phylogenetic analyses and hypothesis testing

We tested hypotheses on the drivers of egg diversification in phasmids following the framework outlined in the introduction and organizing the hypotheses into three classes. All analyses were performed in R (v4.1.1).[84] Continuous variables were $\log_{10}$-transformed prior to the statistical analyses. Phylogenetically-corrected generalized least-squares (PGLS) models were run using the R packages "nlme" and "ape" (correlation= "corPagel").[87,88] Pagel's lambda was estimated using maximum likelihood. Significance of the effect of each explanatory variable was evaluated using a type I (sequential) analysis of variance (ANOVA) or analysis of covariance (ANCOVA). The significance of interaction terms was systematically tested, and non-significant interaction terms ($p<0.05$) were removed from the final models to improve the estimation of intercepts and effect sizes. When appropriate, post hoc pairwise comparisons were run to contrast the intercepts and/or slopes of different levels of a categorical explanatory variable (*emmeans* and *emtrends*:"emmeans")[89] using the Holm method to account for multiple testing.

First, we investigated hypotheses related to the effect of life history strategies on egg size. We tested whether egg size was dependent on adult female size, whether egg size traded off with egg number, and whether females varying in oviposition mode (i.e., parental care investment) varied in reproductive allocation strategy (Table S2). We examined the scaling relationships between adult female size and egg volume and fecundity by running PGLS regressions including lifetime fecundity or egg volume as the response variables and female body volume and oviposition mode as the explanatory variables. Then, to specifically test for a trade-off between egg number and size, we ran a PGLS model including fecundity as the response variable and female body and egg volume as explanatory variables, predicting a negative effect of egg volume on fecundity after accounting for female body size. We then compared the total reproductive output of females as a function of female body volume and oviposition mode, predicting that females investing more energy in parental care (by burying or gluing eggs to specific plants or substrates) would have relatively lower reproductive output. Finally, we tested whether larger eggs developed more slowly than smaller eggs by building a PGLS model including the temperature-corrected duration of embryogenesis as the response variable and egg volume and oviposition mode as predictors.

Next, we tested hypotheses related to mechanical and geometric constraints on egg size and shape (Table S3). When egg size increases, eggs may become wider to save on costly eggshell material, leading to a hyperallometric relationship between egg width and length (i.e., slope greater than 1 on a log-log scale). Alternatively, as they get larger, eggs may become more elongated to be able to fit through a narrow opening during oviposition, to increase their surface area to volume ratio to obtain relatively more oxygen, and/or to minimize diffusion distances between the surface and the central tissues. In this case, we expect a hypoallometric relationship between egg width and egg length (i.e., slope lower than 1 on a log-log scale). We examined the scaling relationship between egg width and egg length using a PGLS regression including egg width as the response variable and egg length and oviposition mode as explanatory variables. Slopes were compared to isometry using 95% confidence intervals. We also tested the scaling relationship of egg surface area and egg size by including egg surface area as the response variable and egg volume and oviposition mode as explanatory variables in a PGLS model. Finally, we examined the relationship between egg width and the width of the female's ninth tergite (where the opening of the oviduct is located) by running a PGLS model including egg width as the response variable and female ninth tergite width and oviposition mode as the explanatory variables. To investigate whether females with relatively narrower abdomen tips laid relatively more elongated eggs, we obtained measures of egg width relative to egg length, and of female ninth tergite width relative to female size by extracting the residuals of two PGLS regressions. One had egg width as a function of egg length and the other had ninth tergite width and female volume. Then we ran a PGLS model including residual egg width as a function of residual ninth tergite width and oviposition mode.

Finally, we examined hypotheses related to ecological circumstances (Table 1). Oviposition mode is expected to affect egg size and shape as the conditions experienced by dropped, buried or glued eggs are likely to be very different in terms of exposure to predators, oxygen availability, and desiccation risk. Buried eggs may benefit from being more elongated so that females can insert them more easily into the substrate and so that they have relatively more surface area for gas exchange underground. Glued eggs, by contrast, are expected to have shapes that vary depending on the substrate to which they are glued (e.g., thin grass leaf, bark, broad leaf). Additionally, glued eggs are likely to be more exposed to predators and desiccation than eggs put on or into soil and may therefore be selected to develop more rapidly. We also tested whether flight capacity affected egg size evolution, taking advantage of the numerous transitions between flight-capable and flightless species seen in stick insects.[53–55,104] Because flight is costly,[51] we predicted that the reproductive investment by flying females would be relatively lower. We also looked at the effect of climate on egg size and shape. We hypothesized that drier climates would drive the evolution of rounder, larger eggs to increase total water stores and limit surface area to volume ratio and therefore relative rates of water loss. To test the effect of these ecological variables on egg size, we built a PGLS model including egg volume as the response variable and female body volume, fecundity, oviposition mode, female flight capacity, climate PC1 and PC2 as predictors. Thus, variation in fecundity and female size was accounted for to avoid confounding effects. Then we built similar PGLS models with either egg surface area, egg width, reproductive output and duration of embryogenesis as response variables and respectively egg volume, egg length, female body volume and egg volume as the first predictors to account for size effects. All models then included oviposition mode, female flight capacity, climate PC1 and 2 as predictors.

Phylogenetic path analyses

We used phylogenetic confirmatory path analyses to compare fits of prespecified models of causal hypotheses among variables to our data, while accounting for nonindependence of observations due to phylogenetic relatedness among species (R package "phylopath").[90,105,106] The variables included in the models were egg volume (n=143 species), egg aspect ratio (i.e., length/width; n=142), female lifetime fecundity (i.e., egg number; n=95), adult female body volume (n=142), temperature-corrected embryonic development time (n=118), female relative ninth abdominal segment width (residuals of PGLS regression between adult female ninth tergite width and body volume; n=142), climate PC1 (i.e., temperate versus tropical; n=142), female flight capacity (binary: 1= flight capable, 0= flightless; n=142) and parental care (binary: 1= eggs placed in specific locations (buried or glued), 0= eggs dropped; n=142). All continuous variables (except principal components and residuals) were $\log_{10}$-transformed. Models with different configurations of these variables were compared using the C-statistic Information Criterion corrected for small sample size (CICc) and were considered equivalent if ΔCICc <2. Models were designed to test the existence and directionality of effects between the variables. We started from an initial model including many logical links (arrows) between variables (Figure S5). From this initial model we went through a model selection procedure consisting of two phases. In the first, we produced alternative models by dropping each arrow one by one. All the produced models were then compared, and the arrow drop associated with the best model was applied to all models. The process was repeated until the main model became the best model (lowest CIC_c). In the second phase, we tested the main model produced in phase 1 against alternative models corresponding to different causal hypotheses and that therefore included reversed arrows. We tested seven alternative causal scenarios that reversed the direction of one or more arrows relative to the starting model: (1) variation in climate PC1 is a consequence (rather than a cause) of variation in egg size, female size and abdominal width; (2) variation in egg size is a consequence of variation in egg number; (3) variation in embryogenesis duration is a cause of variation in egg size; (4) variation in female flight capacity is a consequence of variation in egg size, number, female abdomen width and parental care; (5) variation in parental care is a cause of variation in egg number and size; (6) variation in egg shape (aspect ratio) is a cause of variation in egg size; and (7) variation in female abdomen width is a consequence of variation in egg shape and size (Figure S5). Each alternative model was designed not to include any cyclic paths, which are incompatible with path analyses. All the produced models were compared, and the direction changes associated with the best model were applied to all models. The process was then repeated until the main model was equivalent to the best model. At the end of the second phase, the average of the best performing models (ΔCICc < 2) was calculated, and path coefficients were averaged only over models where the path exists (avg_method="conditional").[90]

It should be noted that path analyses are a statistical tool that evaluate whether the correlational structure of the data is consistent with prespecified causal models, and therefore cannot prove causal relationships.[107] They also do not accommodate feedback loops which are likely in evolution.[108] Therefore, the directionality of the inferred causal effects must be interpreted cautiously.

Analysis of metabolic data

Data were extracted and analyzed using R (v4.1.1).[84] The raw data files contained the relative concentration of CO_2 (parts per million, ppm) inside cell B compared with cell A (the reference cell) according to time (sampling frequency: 1 Hz). We converted raw measures (ppm) to molar rates of CO_2 production ($\dot{M}CO_2$) using measured flow rates inside each chamber (which varied from 10 to 25 ml.min^{-1}) and the Ideal Gas Law:

$$\dot{M}CO_2 = \frac{P\,F\,\Delta[CO_2]}{RT}$$

where Δhe_2 is the rate of CO_2 production (mol.min^{-p}), $\Delta[CO_2]$ is the fractional concentration of CO_2 in cell B relative to cell A, F is the flow rate (L.min^{-i}), P is pressure (1 atm), R is the gas constant (0.08206 L.atm.K^{-K}.mol^{-m}), and T is the temperature measured by the MAVEn (K). Using custom scripts in R, we corrected the CO_2 traces for baseline drift by subtracting the mean baseline values that bracket each set of two experimental chambers.

In general, egg metabolic rate increased continuously during development (Figure 5A), which raises the questions of what representative values to use in other analyses. We approached this problem in three ways. First, for each egg, we estimated the metabolic rate halfway through the total developmental time from cubic regression splines and general additive models (GAM, *gam*: "mgcv", k=5, bs= "cr")[91] fitted to the developmental trajectory of metabolism of each egg separately (Figure S6). Second, we recovered the maximum from these individual trajectories to provide a measure of maximum metabolic rate, which estimates metabolic rate right before hatching. Finally, for each egg, we estimated the total CO_2 produced over its developmental period by integrating rates of CO_2 production at each time point estimated by the GAM and multiplying that value by the total development time. A measure of mean metabolic rate was then obtained by dividing total CO_2 produced by development time.

We tested the scaling relationships of mid-development, maximum and mean egg metabolic rate with egg mass by running linear mixed-effects regressions (*lmer*: "lme4")[92] including species ID as a random effect (Table S4). Variables were $\log_{10}$-transformed prior to analyses. 95% confidence intervals were computed to compare the estimated slope to isometry (slope β= 1). We then investigated how the total CO_2 produced during embryogenesis (i.e., a proxy for the total energy for embryogenesis) varied with egg mass by running a similar linear mixed-effect model (Table S4).

Analysis of rates of water loss data

We tested the scaling relationships of egg water loss rate and initial egg water content with initial egg mass by performing a linear mixed-effects regression after $\log_{10}$-transformation, including species ID as a random effect (Table S4). The effect of oviposition mode was added in the model with water loss as it appeared to have a large effect. For each species, we calculated an average rate of mass loss using a linear mixed-effects regression between egg mass and time, including egg ID as a random effect.

Current Biology, Volume *34*

Supplemental Information

Resource allocation strategies and mechanical constraints drive the diversification of stick and leaf insect eggs

Romain P. Boisseau and H. Arthur Woods

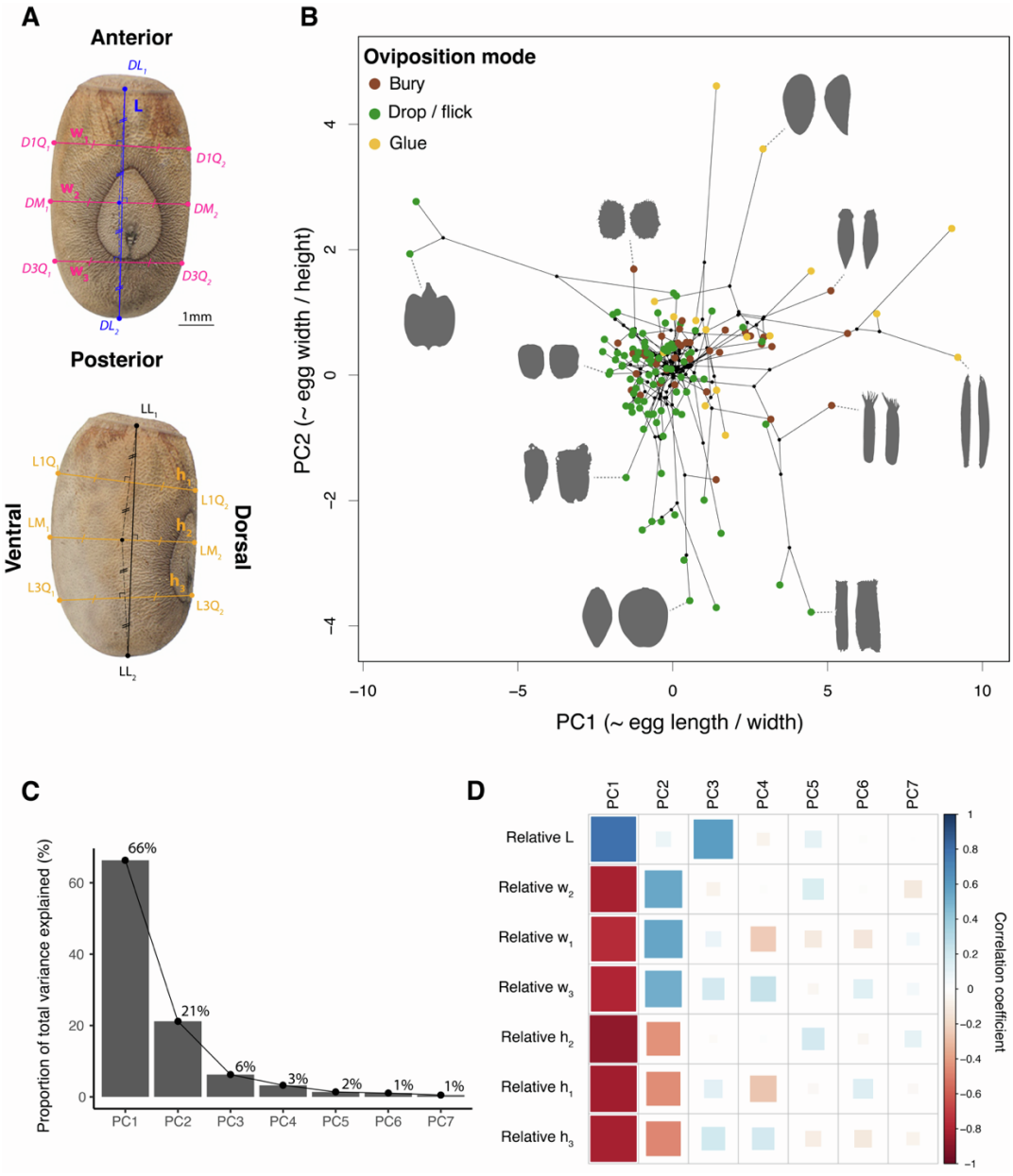

Figure S1. **Phasmid egg measurements and principal component analysis (PCA) summarizing variation in egg shape. Related to Figure 3 and STAR Methods/Method details/Egg morphology**. **A**, Example of guided landmark-based measurements of egg shape traits on two photographs of eggs of *Eurycantha insularis* in dorsal (top) and side (bottom) view following the method of Church, Donoughe et al. (2019)[S1]. **B**, Phasmid egg morphospace showing the two first principal components. Black lines between points represent the underlying phylogenetic relationships between species. Egg silhouettes are represented in dorsal (left) and side (right) view. **C**, Proportion of the total variance explained by each principal component of the egg shape PCA. **D**, Correlation plot showing the extent and direction of the correlations between each principal component (PC) and the egg shape variables included (i.e., residuals of PGLS regressions against egg volume).

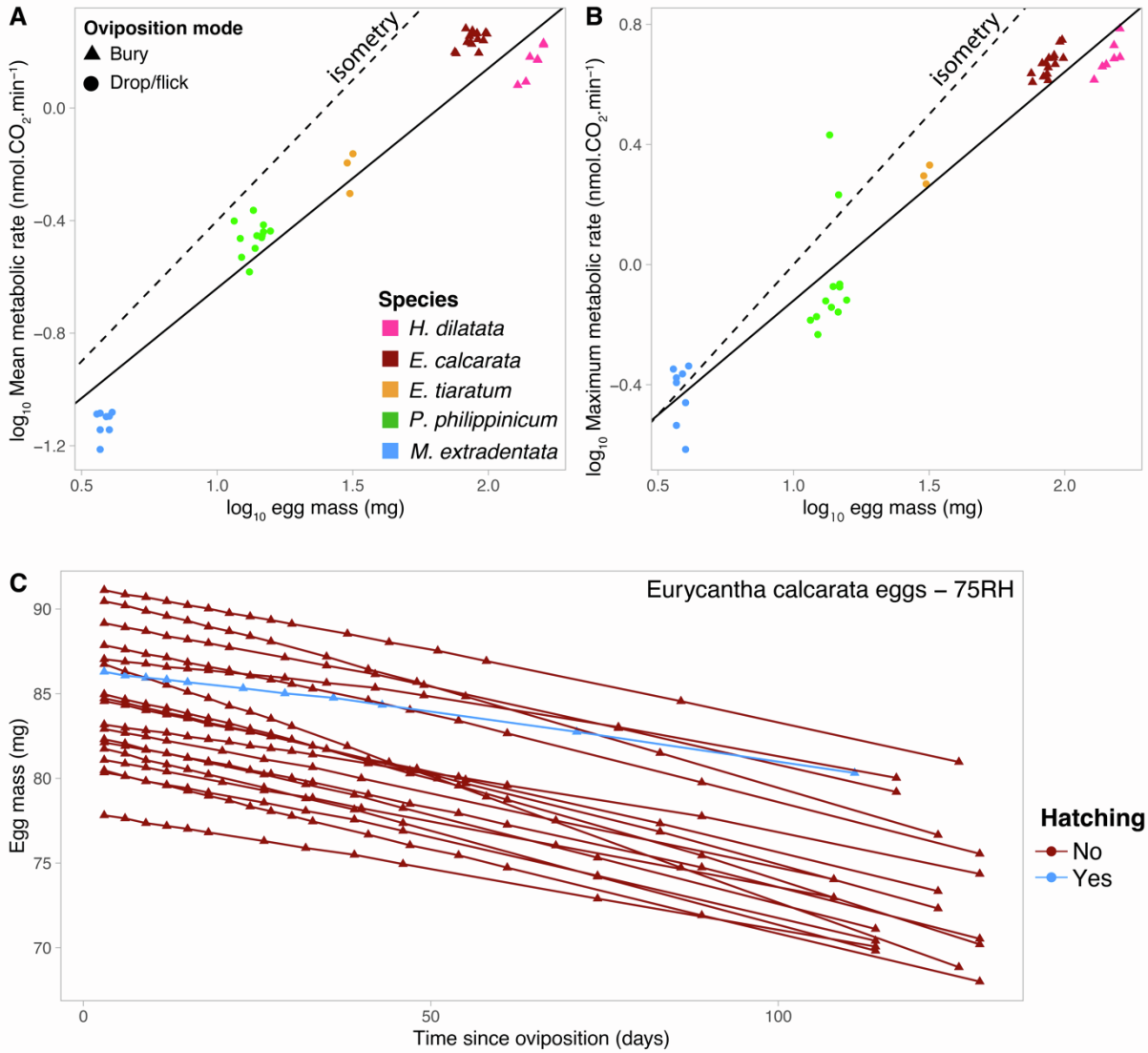

Figure S2. **Metabolic rate allometries and water loss trajectories. Related to Figure 5. A,** Estimated mean and **B,** maximum metabolic rate compared to egg mass. Colors represent the five different species and shapes represent oviposition modes (see legend). Dashed lines represent isometry (arbitrary intercept). Solid black lines represent linear mixed-effects regressions (see table 4 for details on the statistical analyses). **C,** (related to STAR Methods/Method details/Egg rates of water loss) Mass changes of individual eggs of *Eurycantha calcarata* held at 75% relative humidity. Only egg successfully hatched (blue), others never hatched after being monitored for an additional 100 days following the experiment.

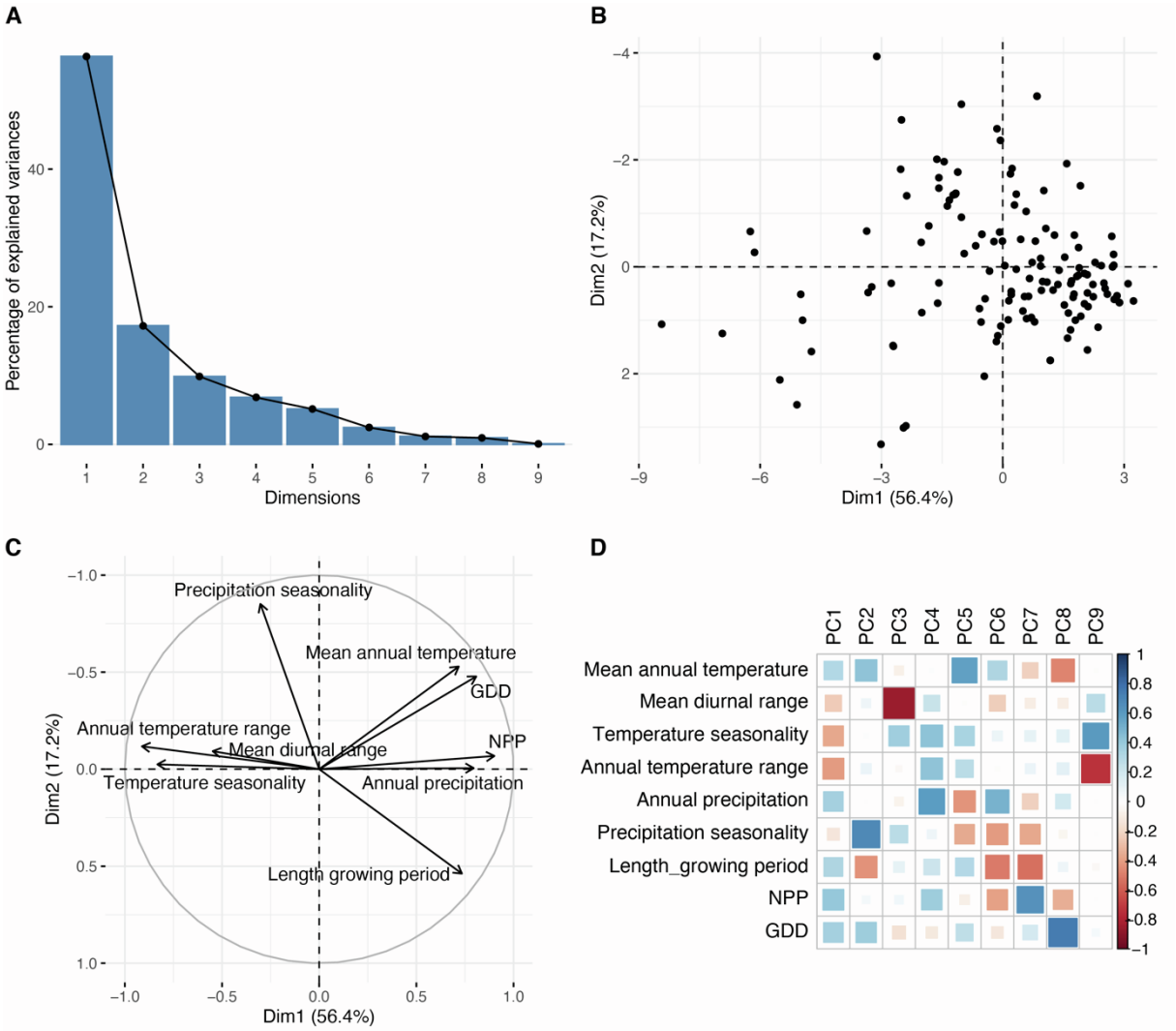

Figure S3. **Principal component analysis (PCA) summarizing variation in climatic conditions experienced by phasmid species**. **Related to STAR Methods/Method details/Ecological data**. **A**, Proportion of the total variance explained by each principal component. **B**, PC2 against PC1 for each species included. **C**, PCA loading plot showing how strongly each climatic variable influences PC1 and PC2. **D**, Correlation plot showing the extent and direction of the correlations between each principal component (PC) and the climatic variables included.

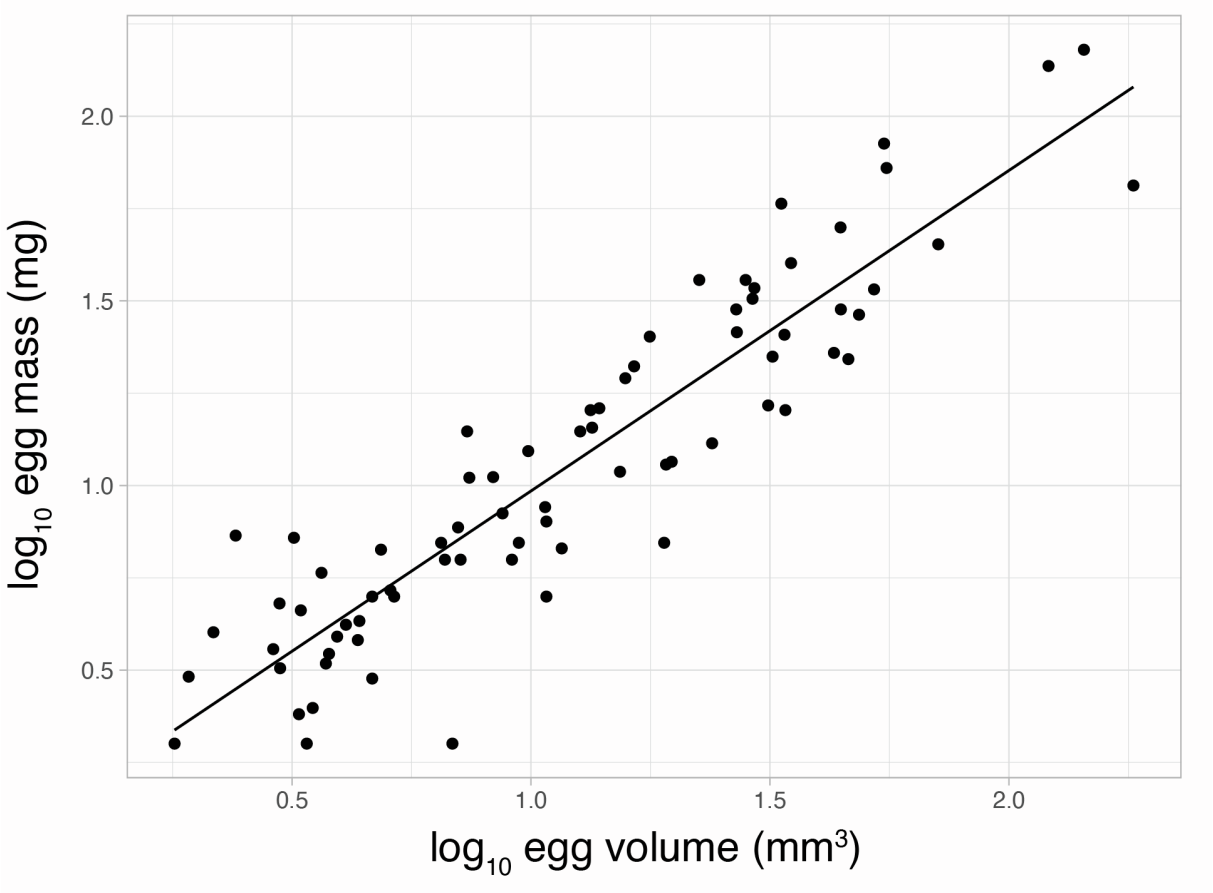

Figure S4. **Egg mass as a function of egg volume across phasmid species**. **Related to STAR Methods/Method details/Egg morphology**. PGLS: β=0.87 $\pm$ 0.04, p<0.0001, R^2=0.84.

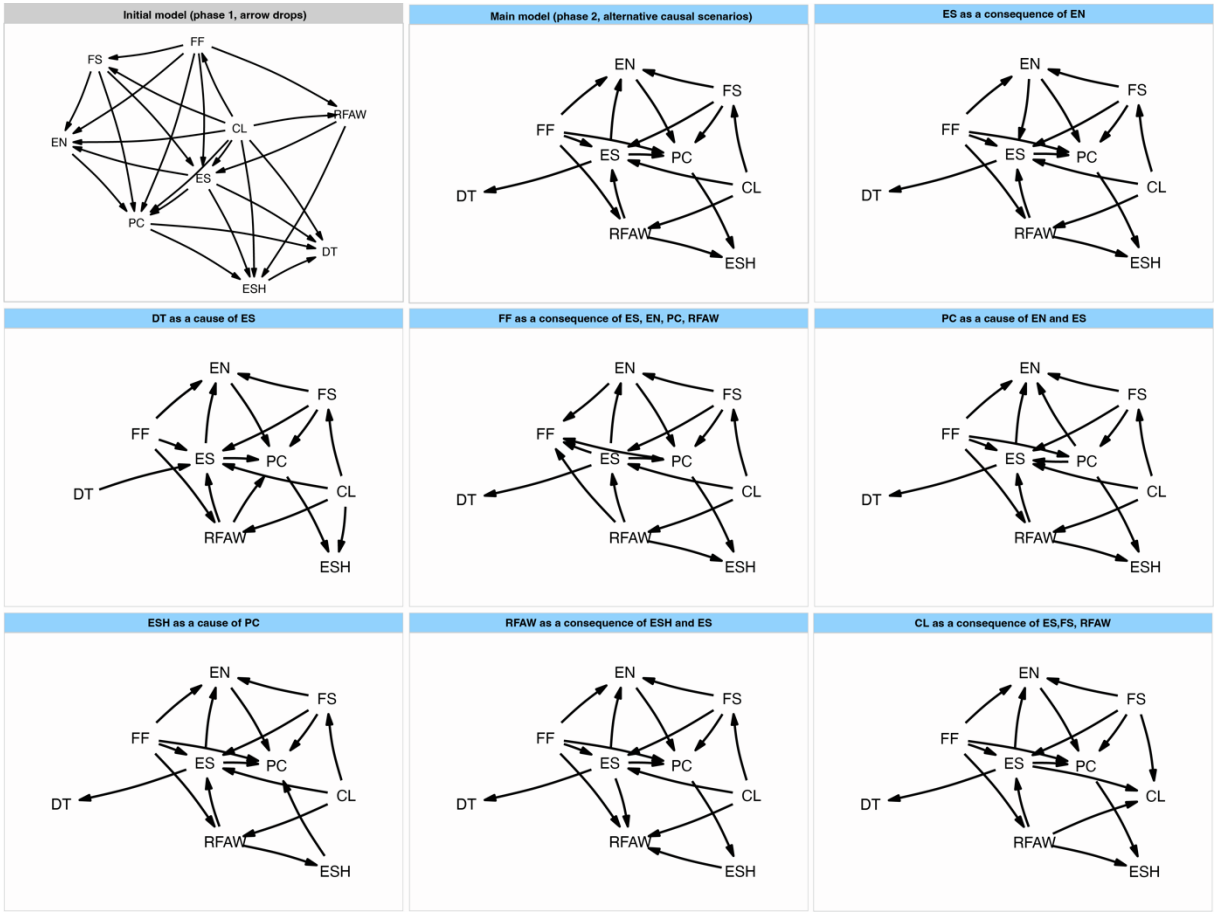

Figure S5. **Path models used as starting point for the two phases model selection procedure. Related to STAR Methods/Quantification and statistical analysis/Phylogenetic path analyses**. The initial model (grey) was used as starting point for the first phase of the model selection procedure which consisted in dropping unsignificant arrows one by one. The main model (blue) was the model resulting from phase 1 to initiate phase 2. It was tested against alternative models corresponding to different causal hypotheses (blue) which included reversed arrows. Arrows show the direction of the path. FF: Female Flight ability; EN: lifetime Egg Number laid by a single female; CL: Climate PC1 (i.e., temperate versus tropical); RFAW: Relative Female Abdomen Width; FS: Female size; ES: Egg Size; PC: Parental Care; ESH: Egg SHape (i.e., egg length/width); DT: egg Development time (temperature-corrected).

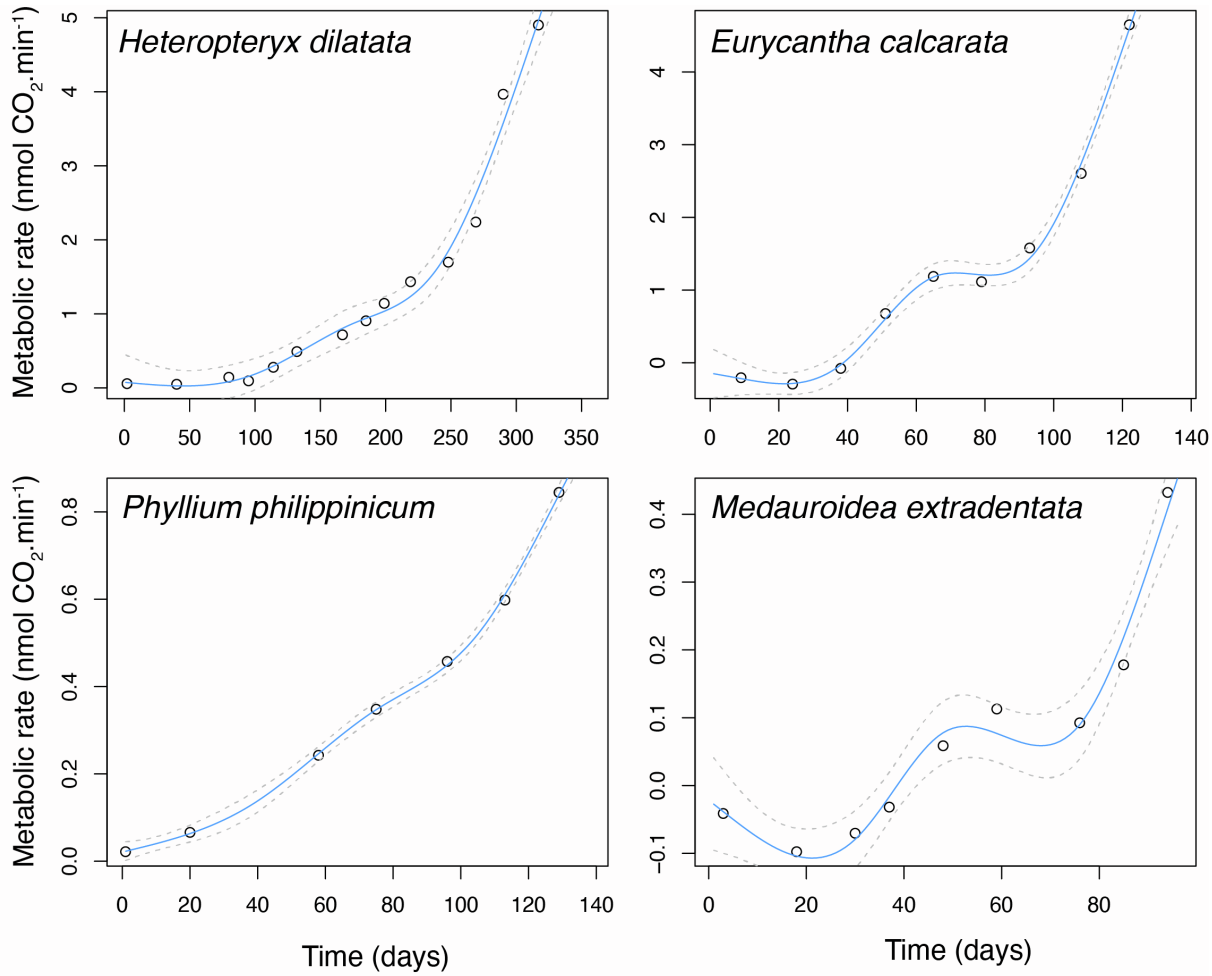

Figure S6. Changes in metabolic rate of individual eggs of four phasmid species during embryonic development. Related to STAR Methods/Quantification and statistical analysis/Analysis of metabolic data. General additive models (cubic regression splines) are fitted to the developmental trajectory.

Egg number	Species	Picture source
1	*Timema californicum*	R. P. Boisseau
2	*Dinophasma saginatum*	F. Tetaert, phasmatodea.fr
3	*Abrosoma festinatum*	F. Tetaert, phasmatodea.fr
4	*Alienobostra brocki*	F. Tetaert, phasmatodea.fr
5	*Cranidium gibbosum*	F. Tetaert, phasmatodea.fr
6	*Ocnophiloidea regularis*	F. Tetaert, phasmatodea.fr
7	*Oreophoetes peruana*	F. Tetaert, phasmatodea.fr
8	*Diapheromera femorata*	F. Tetaert, phasmatodea.fr
9	*Pseudosermyle phalangiphora*	F. Tetaert, phasmatodea.fr
10	*Agathemera crassa*	Cubillos, C., & Vera, A. (2020). Comparative morphology of the eggs from the eight species in the genus *Agathemera* Stål (Insecta: Phasmatodea), through phylogenetic comparative method approach. Zootaxa, 4803(3), 523-543.
11	*Paraprisopus antillarum*	F. Tetaert, phasmatodea.fr
12	*Prisopus berosus*	A.Aiello, STRI_ENT_0103064, Synoptic Insect Collection, Smithsonian Tropical Research Institute, Panama
13	*Creoxylus spinosus*	F. Tetaert, phasmatodea.fr
14	*Anisomorpha buprestoides*	F. Tetaert, phasmatodea.fr
15	*Malacomorpha jamaicana*	F. Tetaert, phasmatodea.fr
16	*Pseudophasma velutinum*	F. Tetaert, phasmatodea.fr
17	*Peruphasma schultei*	F. Tetaert, phasmatodea.fr
18	*Dares validispinus*	F. Tetaert, phasmatodea.fr
19	*Epidares nolimentangere*	F. Tetaert, phasmatodea.fr
20	*Orestes mouhotii*	F. Tetaert, phasmatodea.fr
21	*Haaniella erringtoniae*	F. Tetaert, phasmatodea.fr
22	*Heteropteryx dilatata*	F. Tetaert, phasmatodea.fr
23	*Aretaon asperrimus*	F. Tetaert, phasmatodea.fr
24	*Mearnsiana bullosa*	F. Tetaert, phasmatodea.fr
25	*Bacillus rossius*	F. Tetaert, phasmatodea.fr
26	*Clonopsis gallica*	F. Tetaert, phasmatodea.fr
27	*Parectatosoma mocquerysi*	F. Tetaert, phasmatodea.fr
28	*Achrioptera manga*	F. Tetaert, phasmatodea.fr
29	*Achrioptera punctipes*	F. Tetaert, phasmatodea.fr
30	*Phyllium philippinicum*	F. Tetaert, phasmatodea.fr
31	*Cryptophyllium celebicum*	F. Tetaert, phasmatodea.fr
32	*Pulchriphyllium bioculatum*	F. Tetaert, phasmatodea.fr
33	*Paramenexenus laetus*	F. Tetaert, phasmatodea.fr
34	*Spinohirasea bengalensis*	F. Tetaert, phasmatodea.fr
35	*Phaenopharos herwaardeni*	F. Tetaert, phasmatodea.fr
36	*Lopaphus sphalerus*	F. Tetaert, phasmatodea.fr
37	*Anarchodes annulipes*	F. Tetaert, phasmatodea.fr
38	*Diesbachia tamyris*	F. Tetaert, phasmatodea.fr
39	*Sipyloidea biplagiata*	F. Tetaert, phasmatodea.fr
40	*Trachythorax maculicollis*	F. Tetaert, phasmatodea.fr
41	*Carausius morosus*	F. Tetaert, phasmatodea.fr
42	*Chondrostethus woodfordi*	F. Tetaert, phasmatodea.fr
43	*Manduria systropedon*	F. Tetaert, phasmatodea.fr
44	*Lonchodes auriculatus*	F. Tetaert, phasmatodea.fr
45	*Staelonchodes amaurops*	F. Tetaert, phasmatodea.fr
46	*Eurycantha insularis*	F. Tetaert, phasmatodea.fr
47	*Eurycantha calcarata*	F. Tetaert, phasmatodea.fr
48	*Bactrododema hecticum*	F. Tetaert, phasmatodea.fr
49	*Venupherodes venustula*	F. Tetaert, phasmatodea.fr
50	*Hypocyrtus scythrus*	F. Tetaert, phasmatodea.fr
51	*Pterinoxylus crassus*	F. Tetaert, phasmatodea.fr
52	*Lamponius guerini*	F. Tetaert, phasmatodea.fr
53	*Diapherodes martinicensis*	F. Tetaert, phasmatodea.fr
54	*Phryganistria heusii*	F. Tetaert, phasmatodea.fr
55	*Phobaeticus serratipes*	F. Tetaert, phasmatodea.fr
56	*Pharnacia ponderosa*	F. Tetaert, phasmatodea.fr
57	*Parapachymorpha spiniger*	F. Tetaert, phasmatodea.fr
58	*Rhamphophasma spinicorne*	F. Tetaert, phasmatodea.fr

59	*Ramulus thaii*	F. Tetaert, phasmatodea.fr
60	*Medauroidea extradentata*	F. Tetaert, phasmatodea.fr
61	*Sceptrophasma hispidulum*	F. Tetaert, phasmatodea.fr
62	*Clonaria conformans*	F. Tetaert, phasmatodea.fr
63	*Macrophasma biroi*	Hennemann, F. H., & Conle, O. V. (2006). Studies on New Guinean giant stick-insects of the tribe Stephanacridini Günther, 1953, with the descriptions of a new genus and three new species of Stephanacris Redtenbacher, 1908 (Phasmatodea:"Anareolatae"). Zootaxa, 1283(1), 1-24.
64	*Tropidoderus childrenii*	F. Tetaert, phasmatodea.fr
65	*Clemacantha goliath*	F. Tetaert, phasmatodea.fr
66	*Eurycnema osiris*	F. Tetaert, phasmatodea.fr
67	*Extatosoma tiaratum*	F. Tetaert, phasmatodea.fr
68	*Acrophylla wuelfingi*	F. Tetaert, phasmatodea.fr
69	*Phasma gigas*	F. Tetaert, phasmatodea.fr
70	*Onchestus rentzi*	F. Tetaert, phasmatodea.fr
71	*Megacrania phelaus*	F. Tetaert, phasmatodea.fr
72	*Ophicrania palinurus*	B. Kneubühler, phasmatodea .com
73	*Monandroptera acanthomera*	F. Tetaert, phasmatodea.fr
74	*Rhaphiderus spiniger*	F. Tetaert, phasmatodea.fr
75	*Asprenas brunneri*	F. Tetaert, phasmatodea.fr
76	*Acanthoxyla geisovii*	F. Tetaert, phasmatodea.fr
77	*Carlius fecundus*	B. Kneubühler, phasmatodea.com

Table S1. List of taxa whose eggs are pictured in Figure 1 and sources of the original pictures. Related to Figure 1. All pictures were used by permission.

Response (n species)	Predictor	λ	$F_{df1,df2}$	P	Effect size ± Standard Error (cont.) or Post-hoc pairwise tests (Holm) (cat.)
log_{10} Lifetime fecundity *(= egg number)* (n = 96)	**log_{10} Adult female body volume**	0	**$F_{1,92}$ = 43.48**	**<.0001**	**0.31 ± 0.05**
	Oviposition mode		**$F_{2,92}$ = 22.68**	**<.0001**	**Drop – bury = 0.35 ± 0.05, p<.0001** **Drop – glue = 0.28 ± 0.11, p=0.023** Bury – glue = -0.07 ± 0.12, p=0.55
log_{10} Egg volume (n = 143)	**log_{10} Adult female body volume**	0.57	**$F_{1,139}$ = 192.2**	**<.0001**	**0.67 ± 0.05**
	Oviposition mode		**$F_{2,139}$ = 15.3**	**<.0001**	**Drop – bury = -0.28 ± 0.05, p<.0001** **Drop – glue = -0.23 ± 0.08, p=0.005** Bury – glue = 0.05 ± 0.08, p=0.55
log_{10} lifetime fecundity (n = 96)	**log_{10} Adult female body volume**	0.11	**$F_{1,93}$ = 37.1**	**<.0001**	**0.63 ± 0.08**
	log_{10} Egg volume		**$F_{1,93}$ = 28.8**	**<.0001**	**-0.51 ± 0.10**
log_{10} Reproductive output (egg number x volume) (n = 96)	**log_{10} Adult female body volume**	0.18	**$F_{1,92}$ = 266.4**	**<.0001**	**0.92 ± 0.06**
	Oviposition mode		$F_{2,92}$ = 2.32	0.10	Drop – bury = 0.05 ± 0.07, p=0.45 Drop – glue = 0.28 ± 0.13, p=0.11 Bury – glue = 0.23 ± 0.14, p=0.21
log_{10} Duration of embryogenesis (n = 118)	**log_{10} Egg volume**	0.34	**$F_{1,114}$ = 69.2**	**<.0001**	**0.24 ± 0.03**
	Oviposition mode		**$F_{2,114}$ = 6.72**	**0.002**	Drop – bury = -0.05 ± 0.03, p=0.16 **Drop – glue = 0.23 ± 0.06, p=0.001** **Bury – glue = 0.18 ± 0.06, p=0.005**

Table S2. **Life history correlates of egg size. Related to Figure 2.** The table presents the results of phylogenetic generalized least square models. The most likely value of Pagel's lambda (phylogenetic signal) is presented along with type-I (sequential) ANOVA outputs and either estimated effect sizes or post-hoc pairwise comparisons between estimated marginal means using the Holm method to account for multiple testing, respectively for continuous or categorical explanatory variables. Significant effects are bolded ($p<0.05$).

Response (n species)	Predictor	λ	$F_{df1,df2}$	P	Effect size ± Standard Error (cont.) or Post-hoc pairwise tests (Holm) (cat.)
log_{10} Egg width (n = 143)	**log_{10} Egg length**	0.97	**$F_{1,137}$ = 107.6**	**<.0001**	**0.95 ± 0.16**
	Oviposition mode		**$F_{2,137}$ = 7.53**	**0.0008**	Intercept pairwise comparisons: **Drop – bury = 0.10 ± 0.03, p=0.005** **Drop – glue = 0.11 ± 0.04, p=0.005** Bury – glue = 0.02 ± 0.04, p=0.63
	Interaction		**$F_{2,137}$ = 8.65**	**0.0003**	Slope pairwise comparisons: Drop – bury = -0.20 ± 0.18, p=0.25 **Drop – glue = 0.87 ± 0.23, p=0.0005** **Bury – glue = 1.08 ± 0.27, p=0.0003**
log_{10} Egg surface area (n = 143)	**log_{10} Egg volume**	1	**$F_{1,137}$ = 3913**	**<.0001**	**0.64 ± 0.02**
	Oviposition mode		$F_{2,137}$ = 2.78	0.07	Intercept pairwise comparisons: Drop – bury = -0.02 ± 0.01, p=0.16 Drop – glue = -0.02 ± 0.02, p=0.84 Bury – glue = 0.005 ± 0.02, p=0.84
	Interaction		$F_{2,137}$ = 1.08	0.34	Slope pairwise comparisons: Drop – bury = 0.03 ± 0.02, p=0.73 Drop – glue = 0.06 ± 0.05, p=0.73 Bury – glue = 0.04 ± 0.05, p=0.73
log_{10} Egg width (n = 143)	**log_{10} Female 9th tergite width**	0.57	**$F_{1,139}$ = 241.7**	**<.0001**	**0.68 ± 0.04**
	Oviposition mode		**$F_{2,139}$ = 6.77**	**0.0016**	**Drop – bury = -0.05 ± 0.02, p=0.03** **Drop – glue = -0.09 ± 0.03, p=0.004** Bury – glue = -0.04 ± 0.03, p=0.35
Residual egg width *(after accounting for egg length)* (n = 143)	**Residual female 9th tergite width** *(after accounting for female volume)*	0.95	**$F_{1,137}$ = 29.15**	**<.0001**	**0.75 ± 0.19**
	Oviposition mode		**$F_{1,137}$ = 7.44**	**0.001**	Intercept pairwise comparisons: **Drop – bury = 0.07 ± 0.02, p=0.01** Drop – glue = 0.08 ± 0.04, p=0.06 Bury – glue = 0.006 ± 0.04, p=0.86
	Interaction		**$F_{1,137}$ = 4.33**	**0.015**	Slope pairwise comparisons: **Drop – bury = -0.51 ± 0.21, p=0.048** **Drop – glue = -0.43 ± 0.19, p=0.048** Bury – glue = 0.08 ± 0.24, p=0.73

Table S3. **Allometric scaling of egg shape and mechanical constraints. Related to Figure 3.** The table presents the results of phylogenetic generalized least square models (PGLS). The most likely value of Pagel's lambda (phylogenetic signal) is presented along with type-I (sequential) ANOVA outputs and either estimated effect sizes or post-hoc pairwise comparisons between estimated marginal means using the Holm method to account for multiple testing, respectively for continuous or categorical explanatory variables. Residual egg width corresponds to the residuals of a PGLS regression between egg width and egg length and therefore represents a measure of aspect ratio with lower values indicating more elongated eggs. Residual female ninth tergite width (i.e., the putative maximum diameter of the oviduct opening) corresponds to the residuals of a PGLS regression between ninth tergite width and female volume and therefore represents the relative elongation of the apex of the female's abdomen, with lower values indicating a narrower abdomen. Significant effects are bolded ($p<0.05$).

Response	Fixed effect	Random effect	Effect size ± Standard Error [95% Confidence interval]	Wald χ^2_{df}	P
$\log_{10}$ Mid embryonic development metabolic rate	$\log_{10}$ Egg mass	species	0.70 ± 0.16 [0.36 ; 0.98]	χ^2_1 = 19.9	<.0001
$\log_{10}$ Mean embryonic development metabolic rate	$\log_{10}$ Egg mass	species	0.78 ± 0.10 [0.58 ; 0.97]	χ^2_1 = 62.9	<.0001
$\log_{10}$ Maximum embryonic development metabolic rate	$\log_{10}$ Egg mass	species	0.76 ± 0.06 [0.65 ; 0.87]	χ^2_1 = 178.3	<.0001
$\log_{10}$ Total CO_2 produced during embryogenesis	$\log_{10}$ Egg mass	species	0.97 ± 0.09 [0.76 ; 1.16]	χ^2_1 = 108.3	<.0001
$\log_{10}$ Water loss rate	$\log_{10}$ Egg mass	species	0.66 ± 0.24 [0.05 ; 1.11]	χ^2_1 = 7.52	0.006
$\log_{10}$ Water loss rate	$\log_{10}$ Egg mass	species	0.29 ± 0.07 [0.15 ; 0.43]	χ^2_1 = 16.0	<.0001
	Oviposition mode		Drop – Bury : -0.81 ± 0.08 [-0.97 ; -0.65]	χ^2_1 = 95.7	<.0001
$\log_{10}$ Water content	$\log_{10}$ Egg mass	species	0.99 ± 0.02 [0.96 ; 1.03]	χ^2_1 = 2867	<.0001

Table S4. **Allometry of egg energy use and water loss**. **Related to Figure 5.** The table presents the results of linear mixed-effects models accounting for species as a random effect. Effect sizes (i.e., scaling exponents) are indicated along with type II ANOVA (Wald χ^2**)** outputs including p-values.

Supplemental Reference

S1. Church, S. H., Donoughe, S., de Medeiros, B. A. S., & Extavour, C. G. (2019). A dataset of egg size and shape from more than 6,700 insect species. *Scientific Data*, *6*(1), 1–11. https://doi.org/10.1038/s41597-019-0049-y